


1-1-2015

# Proteasome Inhibition As A Potential Anti-Breast Cancer Therapy: Mechanisms Of Action And Resistance-Reversing Strategies

Rahul Rajesinh Deshmukh  
*Wayne State University,*

Follow this and additional works at: [http://digitalcommons.wayne.edu/oa\\_dissertations](http://digitalcommons.wayne.edu/oa_dissertations)

 Part of the [Cell Biology Commons](#), [Molecular Biology Commons](#), and the [Pharmacology Commons](#)

---

## Recommended Citation

Deshmukh, Rahul Rajesinh, "Proteasome Inhibition As A Potential Anti-Breast Cancer Therapy: Mechanisms Of Action And Resistance-Reversing Strategies" (2015). *Wayne State University Dissertations*. Paper 1333.

This Open Access Dissertation is brought to you for free and open access by DigitalCommons@WayneState. It has been accepted for inclusion in Wayne State University Dissertations by an authorized administrator of DigitalCommons@WayneState.

**PROTEASOME INHIBITION AS A POTENTIAL ANTI-BREAST CANCER THERAPY:  
MECHANISMS OF ACTION AND RESISTANCE-REVERSING STRATEGIES**

by

**RAHUL R. DESHMUKH**

**DISSERTATION**

Submitted to the Graduate School

of Wayne State University,

Detroit, Michigan

in partial fulfillment of the requirements

for the degree of

**DOCTOR OF PHILOSOPHY**

2015

MAJOR: PATHOLOGY

Approved by:

\_\_\_\_\_  
Advisor

\_\_\_\_\_  
Date

\_\_\_\_\_  
\_\_\_\_\_  
\_\_\_\_\_  
\_\_\_\_\_

© COPYRIGHT

RAHUL R. DESHMUKH

2015

All Rights Reserved

## DEDICATION

*To my Sadguru, who has always care for me and has blessed me with everything. For mybeloved mother, who always wanted me to achieve great things in life. For my father, who helped me pursue higher education. For my sisters Seematai, Dhanashreetai, and Hemangi who always believed, encouraged, supported and guided me. Their strength and courage has always been and still is an inspiration. To my beloved wife, Vaishnavi, whose love, patience, and understanding helped me to make my dream true. For my daughters, Shubha and Roma, for bringing love and happiness into my life. To these people I am most grateful. Thank you for all the love and support you have given me.*

## ACKNOWLEDGEMENTS

My greatest appreciation goes to my advisor Dr. Q. Ping Dou for his time, support and guidance. I have learned a lot from our weekly one-on-one and biweekly lab meetings. I appreciate the many opportunities to write reviews and research articles plus the liberty I was given to come up with new ideas and projects. Your advice and wisdom will always help me throughout my life.

A special thanks to Dr. Todd Leff for guidance in not only research related but other issues too. I would not have come so far if Dr. Leff were not there for graduate student like me. Thanks for always being available on short notices, patiently listening to me and giving me good advice. I really appreciate you!

Thanks Dr. Todi for giving me good suggestions for experiments, constructive criticism, and support. I admire your honest feedback and learned a lot from our discussions during committee meetings. Thanks to Dr. Menq-Jer Lee for raising important questions and providing direction for my research projects.

I would like to thank all of the past and present Dou lab members for your help throughout my graduate studies. I have learned a lot from you.

Thanks to Dr. Manohar Ratnam and Dr. Mugdha Patki for assistance with the DNA and RNA isolation experiments. Thanks to Dr. Bepler and Dr. Patrick for providing A549 and HeLa cells. Thanks to Dr. Sanjeev Banerjee for helping me with transportation and advice about different issues in personal as well as professional life. Thanks to Dr. Seongho Kim for his help with the statistical analysis.

I would like to thank the Wayne State Department of Pathology, Oncology as well as Anatomy and Cell Biology for their financial support and help.

A very special thanks goes to Mrs. Deanna Robb for your love, care, support, and advice. My family and I will be indebted to you forever. You are one of the most amazing people we ever met in life. Thanks to Dr. Michael Shapiro and Mrs. Helen Shapiro for taking care of me when I was in an accident in Baltimore, Maryland. I can never forget your care, love and support. You guys help me keep solid faith in humanity.

I would like to thank the three undergraduate students, Kush Patel, Imad Attar and Raghuram Palepu for their help in proofreading my thesis.

Thanks to my dear friends Dr. Vivek Dave, Dr. Muraly Puttabyatappa, Dr. Deepak Gupta, and Dr. Rahul Haware for advice, help, and support.

I would like to thank my Aunt Mrs. Sheela Chauhan, Uncle Mr. Udaysinh Chauhan, Mother-in-Law Mrs. Shobha Rajput, Father-in-law Mr. Vijaysing Rajput and Brother-in-Law Mr. Aashish Khengar for their love, support and help over the years.

Without the support of all these people mentioned above and countless others, I would have never been able to get this far.

## TABLE OF CONTENTS

Dedication	ii
Acknowledgements	iii
List of Figures	v
Chapter 1: General Introduction	1
Breast cancer	1
Ubiquitin proteasome system	1
AMP activated protein kinase	18
Chapter 2: Materials and Methods	29
Chapter 3: Proteasome inhibition induces AMPK activation via CaMKK $\beta$ in human breast cancer cells	
Results	36
Discussion	59
Chapter 4: P-gp or Calcium channel inhibition sensitizes breast cancer cells to proteasome inhibitors	
Results	66
Discussion	85

Chapter 5: Future Directions	88
References	90
Abstract	136
Autobiographical Statement	138



## LIST OF FIGURES

Figure 1: Schematic of Ubiquitin Proteasome System (UPS).....	3
Figure 2: Schematic of AMPK signaling.....	20
Figure 3: Proteasome inhibitors induce AMPK activation in MDA-MB-231 cells.....	37
Figure 4A: Effect of CaMKK $\beta$ inhibition on AMPK activation by proteasome inhibitor, carfilzomib in MDA-MB-468 cells .....	39
Figure 4B: Effects of carfilzomib and STO-609 in MDA-MB-468 cells.....	40
Figure 4C: Effect of CaMKK $\beta$ inhibition on AMPK activation by proteasome inhibitor, bortezomib in MDA-MB-468 cells.....	41
Figure 4D: Effects of bortezomib and STO-609 in MDA-MB-468 cells.....	42
Figure 5A: CaMKK $\beta$ inhibition decreases AMPK activation in LKB1-dysfunctional A549 lung cancer cells.....	44
Figure 5B: Proteasome inhibitory activities of bortezomib in LKB1-dysfunctional A549 lung cancer cells.....	45
Figure 5C: CaMKK $\beta$ inhibition decreases AMPK activation in LKB1-deficient HeLa cervical cancer cells.....	46

Figure 5D: Proteasome inhibitory activities of bortezomib in LKB1 null HeLa cervical cancer cells.....	47
Figure 6A: Intracellular calcium chelation inhibits bortezomib-induced AMPK activation .....	49
Figure 6B: Effects of bortezomib and BAPTA-AM in MDA-MB-468 cells.....	50
Figure 6C: Extracellular Calcium chelation inhibits bortezomib-induced AMPK activation .....	51
Figure 6D: Effects of bortezomib and EGTA in MDA-MB-468 cells.....	52
Figure 7A: CaMKK $\beta$ knockdown decreases AMPK activation induced by bortezomib .....	54
Figure 7B: Proteasome inhibitory activities of bortezomib in MDA-MB-468 cells transfected with scrambled non silencing <i>si</i> RNA or CaMKK $\beta$ <i>si</i> RNA.....	55
Figure 8A: Bortezomib increases newly synthesized CaMKK $\beta$ protein levels.....	57
Figure 8B: qPCR assay to assess CaMKK $\beta$ mRNA levels in bortezomib- or solvent-treated MDA-MB-468 cells.....	58
Figure 9: Proposed schematic for AMPK activation due to proteasome inhibitors.....	60

Figure 10: AMPK activators induce accumulation of ubiquitinated proteins in breast cancer cells .....	62
Figure 11: Verapamil potentiates cytotoxic activities of MG132 in breast cancer cells .....	67
Figure 12: Verapamil potentiates proteasome-inhibitory activities of MG132 in MDA-MB-231 cells .....	70
Figure 13: Verapamil potentiates proteasome-inhibitory activities of bortezomib.....	73
Figure 14: Effect of verapamil on proteasomal activities.....	76
Figure 15: Carfilzomib and verapamil combination induces enhanced cytotoxicity in MDA-MB-231 cells.....	78
Figure 16: Carfilzomib and verapamil combination shows enhanced proteasome inhibition in MDA-MB-468 cells.....	80
Figure 17: Nicardipine enhances cytotoxic activities in MDA-MB-231 cells treated with bortezomib and carfilzomib.....	82
Figure 18: Proposed model for enhanced cytotoxicity due to combination of P-gp and proteasome inhibitors .....	87

## CHAPTER 1

### GENERAL INTRODUCTION

#### Breast Cancer

Breast cancer is the second leading cause of death in women. Triple negative breast cancer (TNBC) is an aggressive subtype of breast cancer. Absence of specific therapeutic targets makes TNBC difficult to treat. Since chemotherapy is the only option, development of new therapeutic strategies to treat TNBC are warranted<sup>1,2</sup>. Ubiquitin-Proteasome System (UPS) and 5'-AMP Activated Protein Kinase (AMPK) have gained significant importance as anti-cancer therapeutic targets. Whether they could be exploited to design new treatment strategies for TNBC needs to be seen. It takes many years and millions of dollars for a new drug entity to get approval from United States (US) Food and Drug administration (FDA) for clinical use<sup>3</sup>. Therefore, repurposing old drugs could be a viable strategy to design new treatments for complex disease such as cancer<sup>4</sup>. While I was testing whether proteasome inhibitors could be repurposed for TNBC, I made an interesting observation that proteasome inhibitors cause AMPK activation in TNBC cells. The mechanism of crosstalk between UPS and AMPK is still not clear; therefore I decided to study it in the TNBC cells. It is important to give background information on UPS and AMPK to fully understand the studies presented here.

#### Ubiquitin Proteasome System

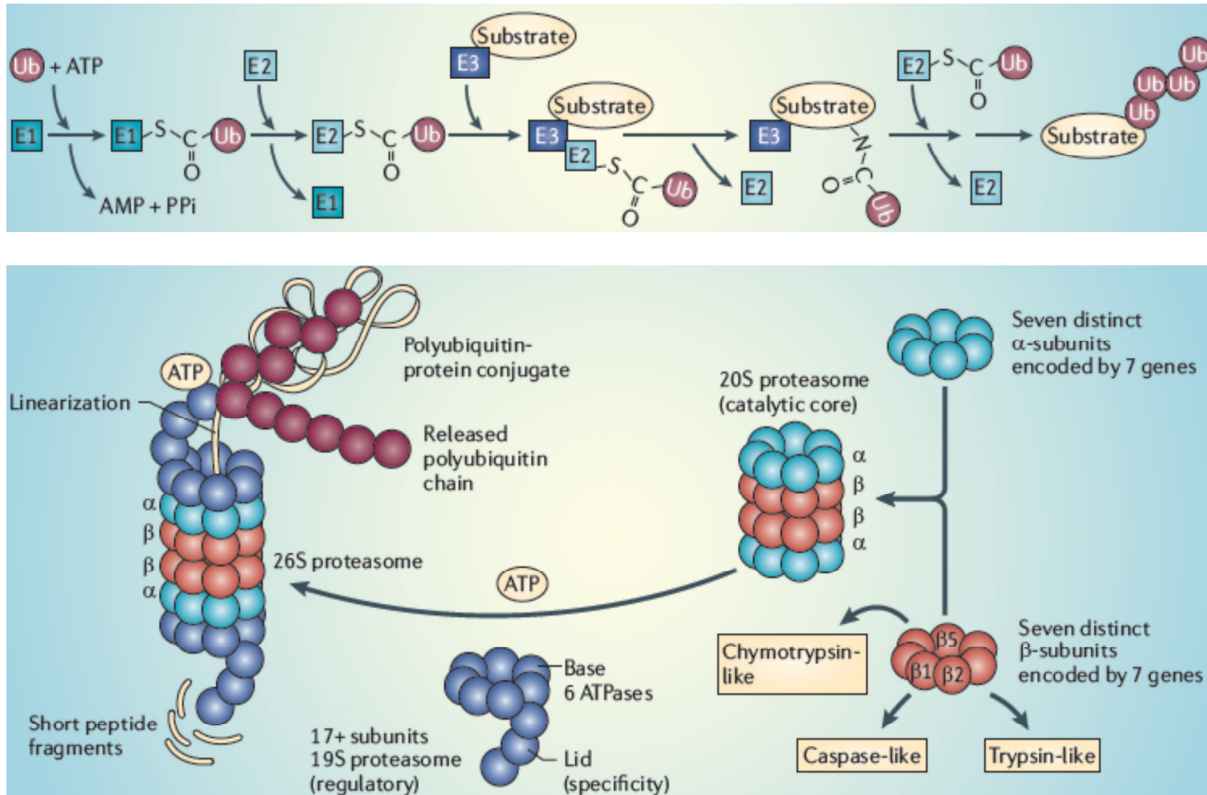
The ubiquitin-proteasome system is responsible for the turnover of the majority of cellular proteins. Therefore, UPS regulates different biological processes, including protein quality control, cell growth, differentiation, proliferation, signal transduction, immune response and apoptosis<sup>5</sup>. Additionally, several non-proteolytic processes, such as transcription initiation and elongation<sup>6</sup>, regulation of gene expression<sup>7</sup> and DNA repair pathways like transcription-coupled nucleotide excision repair<sup>8</sup> are regulated by UPS thus adding another critical layer to

its cellular function. Due to its crucial role in the normal cellular processes and various pathological conditions, Aaron Ciechanover, Avram Hershko and Irwin Rose were awarded the 2004 Nobel Prize in Chemistry for the discoverers of UPS.<sup>9,10</sup>

### **UPS: Structure and Components**

The most important component of UPS, 26S proteasome, a multi-subunit complex (Figure 1) is ubiquitously and abundantly present in cells<sup>11-14</sup>. As demonstrated by in depth biophysical and biochemical studies, the 26S proteasome is composed of the 20S core particle (that possesses proteolytic activities) and one or two 19S regulatory cap particles present on either one or both sides of the core particle<sup>15,16</sup>. The key player, 20S core, is a 28 subunit barrel-like structure of four alternately stacked heptameric rings: two identical  $\alpha$  rings surrounding two identical  $\beta$  rings, each with seven subunits<sup>17-19</sup>. Only unfolded proteins are allowed by  $\alpha$  subunits to enter the 20S core. Various  $\beta$  subunits carry out the highly specific proteolytic activities of the proteasome, depending on an amino-terminal nucleophilic Thr1 residue<sup>19</sup>. Active enzymatic sites on the  $\beta$ 1,  $\beta$ 2, and  $\beta$ 5 subunits are responsible for 20S core proteolytic activities such as caspase or peptidyl-glutamyl peptide-hydrolyzing (PGPH)-like, trypsin (T)-like and chymotrypsin (CT)-like respectively<sup>19-21</sup>. The 19S regulatory cap particle (700 kDa) is comprised of a base and a lid, where the lid is responsible for the deubiquitination of proteasomal substrates before degradation and the base is responsible for the recognition and unfolding of the protein substrates and subsequent opening of the 20S pore along with transport of protein substrates into it. There are six ATPase subunits, Rpt1-6 forming a hexameric ring like structure<sup>22-24</sup>, along with two non-ATPase subunits Rpn-1 and -2<sup>25,26</sup> at the base. The lid is composed of at least six non-ATPases containing ubiquitin interacting motifs (UIMs), including Rpn-10/S5a and Rpn-13/Adrm1<sup>27</sup>. There are two UIMs present on Rpn-10/S5a which preferentially binds poly-ubiquitinated substrates<sup>28</sup>, whereas deubiquitinating enzymes (DUBs) are recruited to the

proteasome by the binding between Rpn-13/Adrm1 and the non-ATPase Rpn-2<sup>29-31</sup>. The process of deubiquitination is an important rate limiting step for ubiquitin-dependent proteasomal degradation as well as recycling ubiquitin molecules, and is tightly regulated<sup>31</sup>.



Q. Ping Dou, Nature Reviews Cancer, December 2011 Vol. 11 No 120

### Figure 1: Schematic of Ubiquitin Proteasome System (UPS).

Initially ubiquitin is activated by an ubiquitin-activating enzyme E1 and transferred to an ubiquitin-conjugating enzyme, E2. The activated ubiquitin is then transferred from E2 to the substrate bound to Ubiquitin ligase E3. The polyubiquitinated substrate is directed to the 26S proteasome where the substrate gets deubiquitinated and unfolded, ultimately leading to its degradation into smaller peptide fragments by catalytic activities of various  $\beta$  subunits of 20S. Ubiquitin=Ub (courtesy from Dr. Q. Ping Dou.)

## **UPS: Mechanism of action**

UPS degrades a protein in two distinct steps: First, multiple ubiquitin molecules are conjugated to the protein substrate, followed by degradation of the ubiquitin-tagged substrate by 26S proteasome. The process of ubiquitination by UPS is performed by three distinct sets of enzymes, E1 (ubiquitin-activating), E2s (ubiquitin-conjugating), and E3s (ubiquitin ligase). Ubiquitin, a small protein comprising 76 amino acids is expressed ubiquitously and serves as a tag for protein substrates resulting in the degradation by the UPS pathway as well as protein kinase activation, membrane-trafficking, DNA repair and chromatin remodeling<sup>32</sup>. First, ubiquitin is activated in a ATP-dependent fashion by E1 enzyme followed by its transfer from E1 to an E2 enzyme, a group of enzymes responsible for ubiquitin conjugation, and subsequently to an E3 ubiquitin-ligating enzyme, which ultimately helps in the transfer of active ubiquitin to lysine residues within the target protein<sup>33,34</sup>. Most of the protein substrates for UPS require conjugation of ubiquitin chain comprising at least four ubiquitin molecules except in few cases such as ODC and HIF-1 $\alpha$ , which require no ubiquitination for proteasomal degradation<sup>35-37</sup>. Following the ubiquitin chain conjugation, the protein substrate is recognized, deubiquitinated, and translocated by components of the 19S regulatory cap to the 20S proteasome<sup>38,39</sup>, leading to its degradation into small peptide fragments of 2-23 amino acids and recycling of the ubiquitin molecules<sup>40</sup>. Although this whole process is tightly regulated in normal cells, it is dysregulated under many human pathological conditions such as tumorigenesis<sup>41</sup>, making UPS a promising target for anti-cancer therapy.

## **UPS and Cancer**

Although UPS plays an important role in normal cellular functions, its dysregulation has been implicated in the development, growth and survival of various cancers<sup>42</sup>. Therefore, various UPS components have been explored as potential therapeutic targets for designing and

developing antineoplastic drugs<sup>43</sup>. It has been demonstrated by many preclinical studies that the proteasomal activities are up regulated in various cancers, including colon, prostate and leukemia<sup>44-46</sup>. This indicates that the cancer cells are more dependent on the UPS than normal cells and, therefore, targeting this pathway for the treatment of human cancer could be a viable strategy. Interestingly, it has been shown that inhibition of chymotrypsin (CT)-like activity of the proteasome is associated with the cell cycle arrest and apoptosis<sup>47,48</sup>. Thus, proteasome inhibition strategy might be advantageous in killing cancer cells over normal cells and could result in selective cancer cell death<sup>49</sup> with little toxicity in normal cells. Consistent with this idea, the US Food and Drug Administration has approved proteasome inhibitors bortezomib and carfilzomib for the treatment of relapsed and refractory multiple myeloma and mantle cell lymphoma<sup>50</sup>.

### **UPS inhibitors**

Systematic efforts were taken to discover or design and develop inhibitors for various components of Ubiquitin Proteasome system. These include natural products-based compounds, metal-based compounds, and small molecule inhibitors of proteasome, deubiquitinase and E3 ligases as well as immunoproteasome inhibitors. It should be noted that most of the earlier efforts were focused on development of 20S proteasome inhibitors<sup>50</sup>.

### **Proteasome Inhibitors: Early Inhibitors**

Many preclinical studies were performed before the approval of bortezomib to confirm whether UPS is a viable therapeutic target. The most widely investigated class of early proteasome inhibitors were the peptide aldehydes such as MG-132 (Cbz-leu-leu-leucinal), MG-115 (Cbz-leu-leu-norvalinal) and ALLN (acetyl-leu-leu-norleucinal). Their chemical structures are similar to the proteasome substrates and have ability to inhibit the CT-like activity<sup>51,52</sup>.



Detailed X-ray diffraction studies with ALLN revealed that it forms a hemiacetyl complex with the N-terminal threonine hydroxyl groups present on the catalytic  $\beta$  subunits of proteasome<sup>18,53</sup>. PSI (Cbz-ile-glu(O-t-Bu)-alaleucinal), another member of peptide aldehyde proteasome inhibitor class, inhibited 26S proteasome-mediated proteolysis with no effect on isopeptidase or ATPase activities<sup>54</sup>. The early phase proteasome inhibitors are potent but reversible; for example, MG-132 shows low nanomolar  $K_i$  in purified proteasome, and low micromolar  $IC_{50}$  in cultured cells.<sup>51,52</sup>

Vinyl sulfone peptides, another class of PIs exert potent proteasome inhibitory activity via covalent binding to the hydroxyl groups present on the active site threonine within the  $\beta$  subunits of 20S proteasome<sup>55,56</sup>. Lactacystin, isolated from actinomycetes<sup>57</sup>, is another early generation proteasome inhibitor that in aqueous solution gets converted to its active form, *clasto*-lactacystin  $\beta$ -lactone<sup>58</sup>. This class of natural compounds is structurally different from the peptide aldehydes and offers enhanced specificity. These compounds have a mode of action similar to that of the vinyl sulfones<sup>59,60</sup>. Different preclinical studies have identified other naturally occurring metabolites with proteasome inhibitory properties such as TMC-95A and Argyrin A. TMC-95A is isolated from *Apiospora montagnei* and belongs to cyclic triterpide class of compounds. It can strongly bind to all the three catalytic  $\beta$  subunits with affinity in the low nanomolar range via hydrogen bonds<sup>61,62</sup>. Argyrin A, a cyclic octapeptide isolated from *Archangium gephyra* has shown tumor growth inhibition that is attributed to inhibition of proteasomal degradation of CDK inhibitor p27<sup>kip1</sup><sup>63,64</sup>. Subsequently more compounds with proteasomal inhibitory properties were identified or designed and developed to specifically target the tumor proteasome, paving the path for the approval of bortezomib by US FDA in 2003.

## Proteasome Inhibitors: Clinically Approved

### Bortezomib

Bortezomib (Velcade®) is a dipeptide boronic acid derivative comprising pyrazinoic acid, phenylalanine and leucine in its structure. Numerous preclinical *in vitro* and *in vivo* studies in animals demonstrated bortezomib efficacy against variety of human cancer cells<sup>65-67</sup>. Bortezomib significantly inhibited cell proliferation<sup>65-67</sup> as well as induced apoptosis in a standard NCI-60 screen that included multiple myeloma, prostate, pancreatic, renal and squamous cell carcinomas<sup>68-73</sup>. Additionally, the growth of multiple myeloma xenografts in mice was potently inhibited by bortezomib<sup>74</sup>. Interestingly, bortezomib exerted antitumor activity in both chemoresistant as well as chemosensitive myeloma cells. Combination of a sublethal dose of bortezomib with chemotherapy significantly increased the sensitivity of resistant cells with no effect on normal hematopoietic cells<sup>75,76</sup>. Based on these preclinical and in depth clinical studies bortezomib was approved by the US FDA for the treatment of relapsed multiple myeloma and mantle cell lymphoma in 2003 and 2006, respectively. Although successful in hematological malignancies, bortezomib has limited scope for the treatment of solid tumors<sup>77,78</sup>, limiting its use in the clinic.

With its proteasome inhibitory activity lasting for almost 72 hours after administration, bortezomib is a reversible inhibitor of proteasome<sup>79</sup>. Boronic acid group on bortezomib binds to the threonine hydroxyl group on the active site of the  $\beta$ 5-subunit, leading to proteasome inhibition and, ultimately, cell death<sup>80</sup>. Bortezomib can enter almost all the tissues except brain and adipose, and its plasma distribution occurs within ten minutes of IV injection<sup>81-84</sup>. With its half-life being more than 40 hours, bortezomib is metabolized by intracellular cytochrome p450 via oxidative deboronation<sup>83,85</sup>.

Although the exact anticancer mechanism is yet to be determined, bortezomib shows selectivity for cancer cells over normal cells. This tumor selectivity of bortezomib is probably due

to the greater dependence of cancer cells on the proteasome for rapid turnover of cell cycle regulatory proteins, generation of misfolded or damaged proteins, and up regulation of proteasome activity to maintain malignant phenotype<sup>67</sup>. It is clear from the bortezomib clinical trials that its mode of action differs from currently used chemotherapeutic agents, as almost one third of the patients enrolled for these clinical trials were heavily pretreated with and did not respond to these therapies<sup>86</sup>. Bortezomib targets diverse signaling mechanisms in cancer cells including the NF- $\kappa$ B signaling pathway. NF- $\kappa$ B normally exists as an inactive p50/p65 heterodimer in the cytoplasm bound to its inhibitory protein, I $\kappa$ B. Proteasome-mediated degradation of I $\kappa$ B leads to the NF- $\kappa$ B complex activation and subsequent translocation into the nucleus where it stimulates transcription of variety of genes including insulin-like growth factor-I (IGF-I), survival factors (IAPs, Bcl-X<sub>L</sub>), and cytokines (IL-6, TNF- $\alpha$ ), ultimately resulting in drug-resistance, proliferation, and resistance to apoptosis in cancer cells<sup>87</sup>. Bortezomib can prevent I $\kappa$ B degradation, thus inhibiting NF- $\kappa$ B activation and ultimately leading to suppression of cytokine related gene expression, survival factors and drug-resistance in multiple myeloma cells with upregulated NF- $\kappa$ B activities<sup>75,88</sup>. In contrast, some studies have suggested that the NF- $\kappa$ B pathway may not be important in bortezomib-mediated tumor cell death as mice with human multiple myeloma cell xenograft showed NF- $\kappa$ B activation, rather than inhibition after treatment with bortezomib<sup>89</sup>.

NOXA (meaning "damage" in Latin), a pro-apoptotic member of the Bcl-2 family of proteins is another proposed bortezomib target<sup>90,91</sup>. The tumor suppressor protein p53 directly activates NOXA promoter thus controlling NOXA gene expression, whereas NOXA assists in p53-mediated apoptosis<sup>91</sup>. NOXA upregulation and its subsequent interaction with and inhibition of anti-apoptotic Bcl-xL and Bcl-2 proteins or stimulation of other pro-apoptotic factors results in apoptosis<sup>18,92,93</sup>. Interestingly, when myeloma and melanoma cells were treated with bortezomib, p53-independent induction of NOXA was also observed. Furthermore, *siRNA*

knockdown of NOXA resulted in only 30% to 50% reduction in bortezomib-induced apoptosis<sup>90</sup>. Variety of p53-defective cancer cell lines when treated with bortezomib resulted in NOXA upregulation<sup>94</sup>. Additionally, clinical trials suggest that bortezomib suppresses tumor growth in a p53-independent manner<sup>15,95</sup>. Interestingly, bortezomib selectively induces NOXA in cancer cells, but not in normal cells such as normal melanocytes where NOXA levels do not change even following bortezomib treatment<sup>90,96,97</sup>.

Additional proposed mechanisms of bortezomib-mediated apoptosis include: induction of endoplasmic reticulum (ER) stress and generation of reactive oxygen species (ROS)<sup>98,99</sup>; inhibition of angiogenesis in human myeloma, pancreatic and squamous cell cancer xenografts<sup>73,100</sup>; induction of extrinsic and intrinsic apoptotic pathways via activation of caspases-8 and -9<sup>101,102</sup>; disruption of the interaction between tumor cells and dendritic cells<sup>103</sup>; and activation of the p38 mitogen-activated protein kinase (MAPK) pathway<sup>104</sup>. Thus, to induce apoptosis in cancer cells, bortezomib targets diverse signaling pathways which may vary depending on the cancer cell type.

However, bortezomib suffers from certain drawbacks. It can cause serious toxic effects such as peripheral neuropathy, thrombocytopenia, neutropenia and lymphopenia as well as common side effects like nausea, diarrhea and fatigue. Peripheral neuropathy is the most common adverse effect observed in approximately 40% of patients treated with bortezomib. The therapeutic window for bortezomib is narrow; its therapeutic dose is 1.3 mg/m<sup>2</sup> whereas the dose-limiting toxic effects are observed at 1.5 mg/m<sup>2</sup><sup>269</sup>. Also, some patients are intrinsically resistant or develop resistance to bortezomib eventually<sup>50</sup>. This led to discovery of second generation proteasome inhibitors such as carfilzomib in the hope that they will offer advantages over bortezomib.

## Carfilzomib

Validation of proteasome as a therapeutic target and the clinical success of bortezomib in MM patients led to accelerated approval for the second-in-class proteasome inhibitor carfilzomib (Kyprolis®) by the US FDA in July 2012 for the treatment of patients with MM progressing on or after treatment with bortezomib and an immunomodulatory agent<sup>50</sup>. Carfilzomib is a highly selective, irreversible inhibitor of the CT-like activity of the proteasome. It belongs to peptide epoxyketone class of compounds<sup>105,106</sup>. Interestingly, carfilzomib inhibited the CT-like activity in both the constitutive proteasome as well as the inducible immunoproteasome with IC<sub>50</sub> values in nanomolar range in preclinical studies<sup>107</sup>. Carfilzomib efficiently inhibited growth in cultured cancer cells and tumor xenograft models, with extended proteasome inhibition for more than a week in mice<sup>107</sup>. Additionally, carfilzomib has shown efficacy in bortezomib resistant myeloma cells and patient-derived plasma cells<sup>105</sup>; however, resistance to carfilzomib in some cancer cells has already been observed<sup>108,109</sup>.

## Proteasome Inhibitors: Mechanisms of resistance

Although clinical success has been achieved with proteasome inhibitors in certain hematological malignancies, like most of other chemotherapeutic agents, resistance has emerged as a limiting factor in their continued clinical use. Similar to other chemotherapeutic drugs, resistance to proteasome inhibitors could be either inherent or acquired<sup>110</sup>. When cells exhibit resistance to a drug without prior exposure, it is an example of inherent resistance. Acquired resistance is observed after exposure to a drug due to diverse mechanisms including but not limited to resistance to apoptosis, genetic mutations and over expression of target proteins<sup>111,112</sup>. While various studies have suggested different potential mechanisms, the exact mechanism for resistant to proteasome inhibitors is still unclear<sup>50,109</sup>.

### **Inherent Resistance**

Some newly diagnosed high-risk multiple myeloma patients showed no clinical response following single-agent bortezomib treatment in the clinical trial ECOG E2A02<sup>113</sup>. Bortezomib treatment to relapsed/refractory acute leukemia patients who had progressed on prior treatments resulted in minimal responses<sup>114</sup>. Additionally, when tested in various solid tumors and other hematological malignancies, bortezomib failed to show any clinical benefit<sup>114</sup>. Also, the lack of therapeutic efficacy due to bortezomib as an initial treatment indicates that some tumors may simply be inherently resistant to proteasome inhibitors<sup>50</sup>.

### **Acquired Resistance**

Although little is known about inherent resistance to proteasome inhibitors, various *in vitro* cell-based studies have suggested multitude of potential mechanisms for acquired resistance to proteasome inhibitors on levels of either its downstream effectors or the proteasome itself<sup>115</sup>. The proposed mechanisms of acquired resistance to proteasome inhibitors are discussed as following.

#### **$\beta$ 5 Subunit Overexpression/Mutation**

Almost 60-fold overexpression of proteasomal  $\beta$ 5 subunit (PSMB5) protein was observed when human monocytic/macrophage THP1 cells were treated with increasing concentrations of bortezomib. Furthermore, alanine-threonine mutation at position 49 in the highly conserved bortezomib-binding pocket was found at the over expressed  $\beta$ 5 subunit<sup>116</sup>. The mutation and over expression of  $\beta$ 5 subunit led to resistance to bortezomib as well as cross-resistance to  $\beta$ 5-targeted cytotoxic peptides such as ALLN, MG132, MG262, and 4A6<sup>116</sup>. Interestingly, no significant changes in the baseline CT-like activity were observed and knockdown of the PSMB5 gene restored the sensitivity to bortezomib<sup>116</sup>. When bortezomib

resistant T lymphoblastic lymphoma/leukemia cells were developed from the Jurkat cell line by treating with the increasing concentrations of bortezomib, Ala49Thr mutation as well as mutations at positions 49 and 50, including Ala49Val, Ala49Thr and Ala50Val in the PSMB5 protein were observed<sup>117</sup>. Also, it has been shown that human leukemia K562 cells naturally over express proteasomal  $\beta 5$  subunit and are relatively more resistant to bortezomib than other leukemia and myeloma cell lines. Unfortunately, it is still unknown whether mutations in  $\beta 5$  subunit or its over expression are responsible for bortezomib resistance *in vivo*<sup>118</sup>. Study in a multiple myeloma patient who quickly developed resistance to bortezomib found no mutations in the coding region of PSMB5<sup>119</sup>. Large scale, detailed clinical studies are warranted to determine whether and how  $\beta 5$  mutations as well as over expression contribute in resistance to proteasome inhibitors *in vivo*.

### Upregulation of Heat Shock Proteins (HSP)

It is suggested that the heat shock proteins (HSPs) contribute to resistance to apoptosis. Multiple HSPs, especially HSP-72, are up regulated due to proteasome inhibition<sup>120,121</sup>; for example, treatment with tripeptidyl aldehyde proteasome inhibitors, lactacystin or MG-132 significantly upregulated HSP-72<sup>122-124</sup>. The role of HSP-72 upregulation in resistance to proteasome inhibitors was validated by a study where MG-132 mediated apoptosis was potentiated when combined with HSP-72 knockdown as compared to each agent alone<sup>125</sup>. Also, HSP-72 knock down in prostate cancer cells enhanced MG-132-induced cell death<sup>126</sup>. On the contrary, other studies have demonstrated that proteasome inhibitor-mediated HSP-72 up regulation could be pro-apoptotic<sup>123,124</sup>.

Proteasome inhibition by bortezomib in myeloma cells also induced other HSPs such as HSPs-70, -27, and -90 as shown by gene profiling studies<sup>101,127,128</sup>. It has been shown that bortezomib treatment resulting in p38 activation led to enhanced HSP-27 phosphorylation.

Furthermore, combination of p38 inhibitors and HSP-27 knockdown reversed resistance to proteasome inhibitor<sup>127,129</sup>. A study suggested that HSP-70 contributes to bortezomib resistance<sup>128</sup>. Interestingly, acquired resistance to bortezomib caused by HSP-70 up regulation was diminished due to quercetin mediated inhibition of HSP-70 mRNA and protein expression<sup>130</sup>. Pancreatic cancer cells express high levels of HSP-70 and its inhibition via either quercetin treatment or siRNA knockdown induced apoptosis in the pancreatic cancer cells<sup>131</sup>.

HSP-90 is involved in proper folding of various proteins that contributes to signal transduction pathways. It is also implicated in resistance to proteasome inhibitors<sup>101</sup>. Treatment of breast cancer cells with the combination of an HSP-90 inhibitor and bortezomib resulted in synergistic cell death<sup>132</sup>. Also, HSP-90 inhibitor and bortezomib combination showed enhanced apoptosis in several preclinical multiple myeloma cell models<sup>132-134</sup>, including pancreatic cancer cells; the combination treatment induced necrotic cell death rather than apoptosis<sup>135</sup>. These studies with the combination of proteasome inhibitors and HSP-90 antagonists warrant in depth studies to deduce mechanisms of the combination as well as plausible interactions with each another.

### **Altered Expression of Apoptosis-Related Proteins**

BCL-2 family member proteins such as Bim<sup>136</sup> and NOXA<sup>94</sup> are suggested to be involved in proteasome inhibitor-induced cell death. Although inactivating mutations in these proteins are rare in tumors<sup>137,138</sup>, cancer cells via epigenetic mechanisms can acquire resistance to proteasome inhibitors; e.g. miR-17-92 and NFB2/p52 inhibited Bim expression in some cell types<sup>139,140</sup>; also Noxa expression depends on its gene methylation by Bmi-1<sup>141</sup>. Over expression of anti-apoptotic Bcl-2 proteins may also diminish Noxa and Bim effects<sup>142</sup>. Indeed, small molecule inhibitors for Bcl-2, Bcl-xL (ABT-737) and MCL-1 (obatoclax) ameliorated bortezomib-mediated cell death in different human cancer cell lines<sup>143-145</sup>.



Some studies show that proteasome inhibition resulted in increased levels of pro-apoptotic proteins such as p27 that contribute to cell death<sup>64,146</sup>. Although inactivating mutations in p27 gene are rarely reported, increased Skp2 activity decreases p27 expression and proteasome-mediated degradation<sup>147</sup>. Methylation of p27 gene promoter has been observed in approximately 10% of various types of cancers<sup>148</sup>; furthermore, studies suggest that resistant phenotype in proteasome inhibitor-resistant tumors might be due to enhanced methylation of p27 gene. Additionally, subcellular localization of p27 is altered due to its phosphorylation by AKT<sup>149,150</sup>, and thought to be responsible for acquired resistance to proteasome inhibitors.

### **AKT Pathway Activation**

The PI3K/AKT pathway promotes cell survival and reported to be constitutively active in different types of cancer. PTEN deletion<sup>151</sup>, amplification of PI3K<sup>152</sup> or AKT<sup>153</sup> gene, growth factor receptor signaling<sup>154</sup>, or mutation of Ras family proteins<sup>155</sup> are implicated in abnormal activation of AKT pathway. Bortezomib can cause direct activation of AKT in some cell lines<sup>156</sup>, and none the less, AKT activation, either constitutive or induced, has been shown to hinder the anti-cancer activities of bortezomib<sup>101,157,158</sup>. Direct and indirect inhibitors of AKT signaling such as PI3K inhibitors like perifosine, the Raf inhibitor sorafenib<sup>158</sup>, and the PKC antagonist enzastaurin<sup>159</sup>, have been shown to enhance apoptosis mediated by bortezomib. As receptor tyrosine kinase growth factor receptors such as EGFR also regulates AKT activation, selective RTK inhibitors can reverse AKT activation, resulting in sensitization of cancer cells to bortezomib<sup>160-162</sup>.

### **Over expression of Other Growth-related Proteins**

Some studies have suggested that the over expression of cell growth-promoting proteins such as interleukin-6 (IL-6) and insulin-like growth factor (IGF-1) could subsequently lead to

bortezomib resistance through NF- $\kappa$ B activation via the PI3K/Akt and Raf/MEK/ERK pathways<sup>163,164</sup>. In bone marrow stromal cells (BMSCs), IL-6, via inhibition of miRNA expression, regulates sensitivity to bortezomib in multiple myeloma cells<sup>165,166</sup>. Additionally, multiple myeloma cells over express IGF-1 receptor which in combination with high IGF-1 levels contributes to disease progression and poor patient prognosis<sup>167,168</sup>. Upregulated IGF-1 signaling was observed in multiple myeloma cells with no  $\beta$ 5 mutations and thought to be responsible for resistance to bortezomib. Furthermore, gene expression profiling studies in these bortezomib-resistant multiple myeloma cells showed that genes activated by IGF-1 were constitutively expressed. Importantly, partial reversal of bortezomib resistance was observed when IGF-1 downstream effectors such as PI3-K and mTOR were inhibited. Cultured cells, in vivo models and patient samples were sensitized to bortezomib treatment when IGF-1R was directly inhibited<sup>169</sup>, indicating that bortezomib and IGF-1R inhibitor combination could be a valuable strategy to overcome or prevent resistance to proteasome inhibitors.

### **Altered Autophagy Pathways**

It has been shown that proteasome inhibition leads to autophagy induction as a compensatory response. Although the precise role of autophagy in cancer cell death is still not clear<sup>170</sup>, different studies have shown that autophagy inhibition can both promote<sup>171</sup> or inhibit<sup>172</sup> proteasome inhibitor-induced cell death, depending on the cell type. This could be attributed to the inability of the autophagy inhibitors to inhibit chaperone-mediated autophagy, although they block macroautophagy in some cell types resulting in clearance of protein aggregates via their transfer to the lysosome through aggresomes during chaperone-mediated autophagy. HDAC6 is involved in the process of aggresome formation, hence, HDAC inhibition could be a promising strategy to enhance proteasome inhibitor-induced cell death in cells that are sensitive to proteasome inhibitors as well as to reverse resistance in cells that are resistant to proteasome

inhibitors<sup>173,174</sup>. Due to the promising results from in depth cell based studies, Phase I clinical trials investigating the combination of bortezomib and the pan-HDAC inhibitor SAHA was conducted in patients with relapsed/refractory multiple myeloma<sup>175</sup> as well as solid tumors [NCT00310024; National Cancer Institute]. Also, results of a Phase II trial to investigate this combination in patients with progressive, recurrent glioblastoma are pending [NCT00641706; National Cancer Institute].

### **Increased Antioxidants**

Some studies have suggested that proteasome inhibitors induce production of reactive oxygen species that contribute to their anticancer properties. Therefore, it was hypothesized that antioxidant protection mechanisms could also play role in resistance to proteasome inhibitors. When intracellular reduced glutathione was depleted by buthionine sulfoximine treatment, sensitivity of multiple myeloma cells to bortezomib was enhanced<sup>176</sup>. Glutathione acts as a cofactor for GSH-dependent enzymes (e.g., protein disulfide isomerase, glutathione peroxidase), and thus have the ability to promote resistance to proteasome inhibitors. Vitamin C could also inhibit toxicity induced by proteasome inhibitors<sup>177-181</sup>. Hence, antioxidant levels may affect sensitivity to proteasome inhibitors; therefore regulating the antioxidant levels could be helpful in overcoming the resistance to proteasome inhibitors.

Additionally, general mechanisms of chemoresistance such as alteration in influx or efflux of proteasome inhibitors as well as their inactivation by metabolizing enzymes such as Cytochrome P450 could also be involved in, and used as a target to overcome resistance to proteasome inhibitors.

### **Proteasome Inhibitors: Concluding Remarks**

The clinical approval of proteasome inhibitors bortezomib and carfilzomib was validation of the importance of the ubiquitin proteasome pathway as a critical anticancer therapeutic target. Intrinsic and acquired resistance to clinical proteasome inhibitors has been observed in cancer cells, making it important to find novel ways to overcome the resistance. Resistance may be due to a variety of factors including over expression or mutation of the  $\beta 5$  subunit, over expression of HSPs, altered expression of apoptosis- and growth-related proteins, AKT pathway activation, altered autophagy and increased antioxidant levels. Toward the goal of overcoming this resistance, novel small molecules have been developed in order to selectively target and inhibit different components of ubiquitin-proteasome pathway other than the catalytic 20S core. These novel targets include the 19S regulatory cap, deubiquitinating enzymes and the enzymes involved in the ubiquitination cascade (E1, E2s and E3s). Inhibitors that are derived from natural products as well as those containing metal centers could also be viable choices for overcoming resistance associated with clinical proteasome inhibitors. Finally, immunoproteasome is an inducible form of proteasome under special conditions such as inflammation, which might provide some specificity in terms of its structure as well as substrates. Therefore targeting immunoproteasome could also be an important strategy to overcome resistance to constitutive 20S proteasome.

In conclusion, although the ubiquitin-proteasome system is a promising and valid target for cancer therapy, 20S proteasome inhibitors are only useful in the treatment of selected hematological malignancies and offer no or little hope in the treatment of solid tumors. One potential strategy to overcome this limitation could be the use of other therapeutic agents to sensitize resistant cancer cells to proteasome inhibitors. Also, systematic efforts should be taken to identify and validate additional plausible targets of proteasome inhibitors such as AMPK that might contribute to its anticancer effects.

## AMPK: A Metabolic Switch

AMPK is an evolutionary conserved serine threonine kinase present in all eukaryotic cells. AMPK acts as a switch that regulates energy and metabolic homeostasis at cellular as well as whole organism level<sup>182-184</sup>. It universally exists as heterotrimeric protein complexes (Figure 2) consisting of a catalytic  $\alpha$ -subunit and two regulatory subunits,  $\beta$  and  $\gamma$ <sup>185-187</sup>. The enzymatically functional kinase domain that is responsible for phosphorylation of AMPK substrates is present in the  $\alpha$ -subunit. A highly conserved Threonine, at position 172 (Thr172), serves as a crucial target for phosphorylation by the upstream kinases is situated in the activation loop of AMPK- $\alpha$ <sup>188</sup>. Major upstream kinases that differentially modulate AMPK's activity in response to diverse biological as well as physiological conditions and stimuli are Liver Kinase B1 (LKB1)<sup>188</sup>, Calcium-Activated Calmodulin-Dependent Kinase Kinase  $\beta$  (CaMKK $\beta$ )<sup>189</sup> and Transforming growth factor- $\beta$ -Activated Kinase 1 (TAK1)<sup>190,191</sup>. Phosphorylation of Thr172 located in the activation loop of catalytic AMPK- $\alpha$  subunit is universally required for full activation as well as subsequent induction of downstream AMPK signaling as well as functional consequences and currently used as a biomarker for AMPK activation<sup>192,193</sup>.

The mammalian AMPK  $\alpha$ -catalytic subunit is encoded by two genes, PRKAA1 & PRKAA2, whereas the regulatory  $\beta$  and  $\gamma$ -subunits of AMPK are encoded by PRKAB1 and PRKAB2, as well as PRKAG1, PRKAG2 and PRKAG3, respectively<sup>115,194,195</sup>. The isoforms of AMPK subunits exhibit tissue-specific expression pattern as well as functions<sup>50,195,196</sup>. For example, AMPK- $\alpha$ 2 is preferentially localized in nucleus as compared to the cytosolic AMPK- $\alpha$ 1 localization, although nuclear localization of AMPK- $\alpha$ 1 subunit has been reported under specific experimental conditions<sup>197</sup>. Additionally, the two catalytic AMPK- $\alpha$  subunits show different responses to AMP binding and LKB1 association. Interestingly, differential activities for various isoforms of AMPK- $\beta$  subunits have also been reported<sup>198</sup>. Also, localization to specific

membranes and full activation of the AMPK requires myristoylation of its  $\beta$  isoforms<sup>199</sup>.

### **AMPK Activation**

The canonical AMPK activation mechanism in mammalian cells due to variety of stimuli such as xenobiotics, drugs,<sup>200</sup> and metabolic stresses involves a two-pronged mechanism: First, binding of adenine nucleotide states (AMP/ADP/ATP) to specific regulatory sites on the complex at different subunits and secondly, activation by the specific upstream kinases such as LKB1, CaMKK $\beta$ , and TAK1 (Figure 2)<sup>195</sup>. Interestingly, adenine-nucleotides can bind to three distinct sites present on the AMPK- $\gamma$  subunit with different degrees of affinity<sup>201,202</sup>. A moderate decrease in intracellular ATP leads to a proportionate, concurrent and corresponding increase in intracellular AMP levels ultimately resulting in the enhancement of AMPK activities by 5-fold<sup>203</sup>. Direct binding of AMP to the AMPK- $\gamma$  regulatory subunit has been observed with the additional increases in cellular AMP levels. A conformational change resulting from the binding of AMP to the AMPK- $\gamma$  regulatory subunit leads to enhanced AMPK- $\gamma$  phosphorylation in addition to diminished dephosphorylation at Thr172 ultimately resulting in a >100-fold increase in AMPK activities<sup>204,205</sup>. Some studies suggest that ADP can also bind to the AMPK- $\gamma$  subunit. Therefore, intracellular ADP levels may also contribute to AMPK activation in response to variety of metabolic states and cellular stresses<sup>206</sup>. Finally, irrespective of its mode of activation, AMPK, upon activation, switches off the biosynthetic pathways that consume energy while switching on catabolic pathways that generate energy, thus maintaining cellular energy homeostasis<sup>207</sup>.

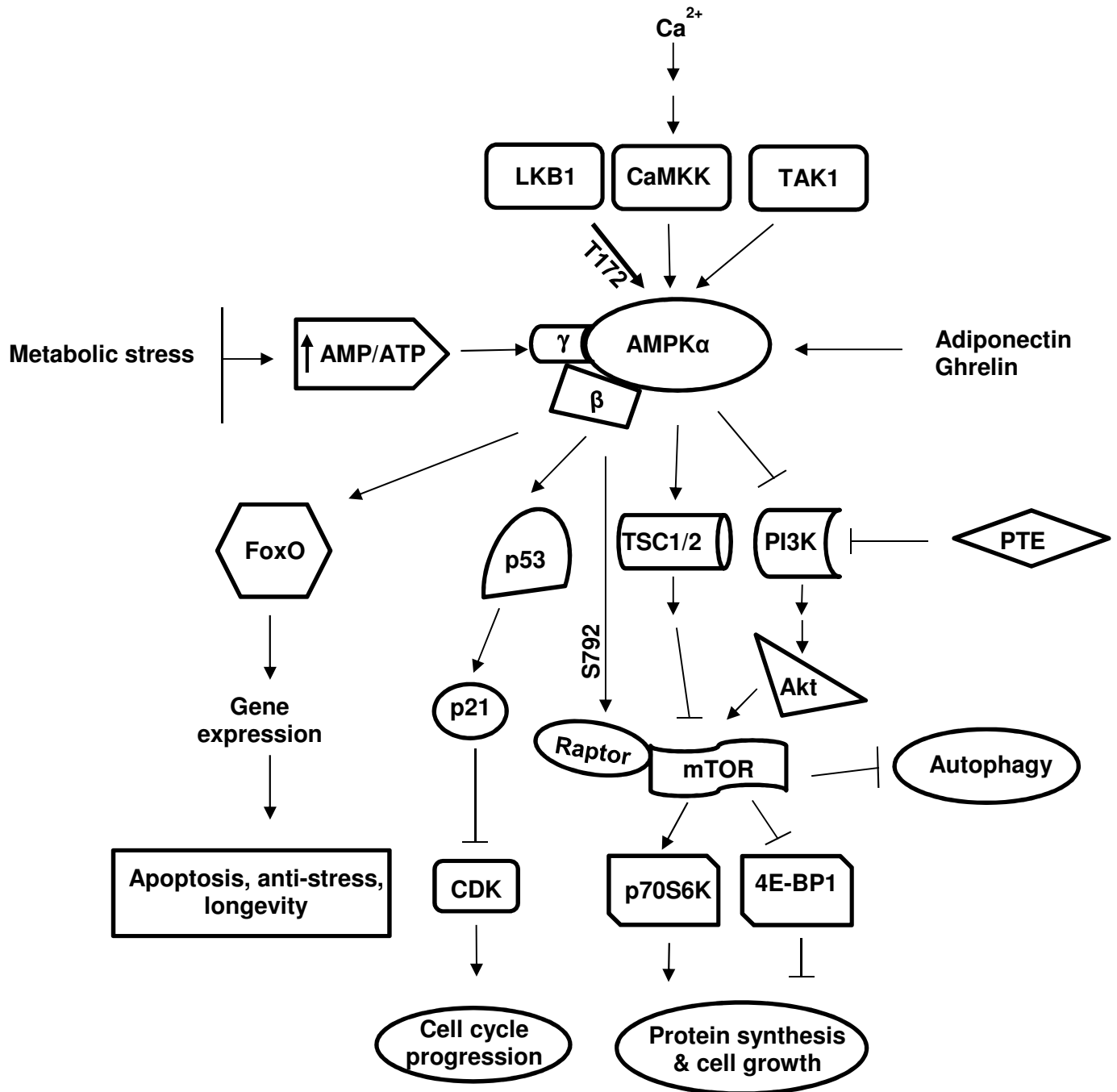


**Figure 2: Schematic of AMPK signaling.** AMPK universally exists as a trimeric complex. AMPK is activated by various stimuli such as elevated AMP/ATP ratio due to metabolic stress, upstream activators and enzymes such as adiponectin, ghrelin. AMPK activation leads to various cellular events such as inhibition of mTOR signaling. (Courtesy from Dr. Di Chen, Karmanos Cancer Institute)

### **AMPK Signaling: Diverse and Multifaceted**

AMPK-mediated signaling is regulated by various upstream kinases including LKB1. LKB1 is a serine/ threonine kinase encoded by the gene STK11 and functions as a tumor suppressive protein<sup>208-210</sup>. AMPK, a major downstream effector of LKB1 gets phosphorylated at Thr-172 in  $\alpha$  subunit and has been suggested to be responsible for many of LKB1's important tumor suppressive activities such as inhibition of mTORC1 signaling<sup>211</sup>. Under normal physiological conditions, LKB1 is in constitutively active form and plays various roles in cellular processes such as proliferation, survival, polarity, and metabolism. The high basal activities of LKB1 are critical and required for AMPK activation in response to AMP and/or ADP binding to the AMPK- $\gamma$  subunit<sup>212</sup>. Additionally, LKB1 as well as its downstream substrates, such as AMPK-related kinases, might be involved in various phenotypes of LKB1-deficient tumors. Some studies have suggested that ROS can also activate AMPK independent of LKB1 status. Hence, although AMPK and LKB1 signaling appears to be closely related, there are significant variations in their signaling in the context of inhibition of tumorigenesis<sup>213</sup>.

Although LKB1 is the major upstream kinase for AMPK, another Serine-Threonine kinase named CaMKK $\beta$  (CaMKK2) can also phosphorylate AMPK- $\alpha$  at Thr172, in response to intracellular calcium modulations and in a LKB1- and energy state-independent manner<sup>214</sup>. CaMKK $\beta$ , a 66-68 kDa protein, is a member of Ca<sup>2+</sup>/calmodulin-dependent protein kinases (CaMKs) family. The CaMK signaling cascade is activated due to increase in intracellular calcium (Ca<sup>2+</sup>) levels either from opening of ligand- or voltage-gated channels or alternatively via release from intracellular stores such as endoplasmic reticulum. Ca<sup>2+</sup> then binds to its intracellular, ubiquitous receptor calmodulin (CaM) with high affinity forming a complex that subsequently binds and activates CaMKs. Mammalian CaMKK $\beta$  exists in two isoforms namely, CaMKK $\alpha$  and CaMKK $\beta$ . CaMKK $\beta$  is marked by the presence of unique regulatory domain



composed of overlapping autoinhibitory and CaM-binding regions that follows central serine threonine kinase domain. Diverse stimuli such as binding of antigens to T-cell receptor, binding of endogenous and exogenous cannabinoids to the cannabinoid receptor (CB2), thrombin in endothelial cells as well as ghrelin (the hunger hormone) activities in hypothalamic neurons can increase intracellular levels of  $Ca^{2+}$ , resulting in AMPK activation<sup>215-217</sup>. Additionally, the MAPKKK family member TAK1/MAP3K7 can also activate AMPK by phosphorylating AMPK- $\alpha$  at Thr172 where whether LKB1 or CaMKK $\beta$  plays role in it is still not clear<sup>218</sup>. These studies demonstrate that AMPK signaling is very complex due to various stimuli and complex network of regulatory molecules that modulate AMPK activity. Furthermore, the cross talk between AMPK and AMPK-related kinases adds another layer of complexity warranting in depth studies to understand how this master regulator functions in normal and cancer cells so that specific targeted therapies and drugs could be developed to target the AMPK signaling pathway<sup>219</sup>.

AMPK modulates energy homeostasis at cellular as well as organismal level by the directly regulating enzymes involved in metabolism through their phosphorylation<sup>220</sup>. AMPK activation results in inhibition of energy-consuming processes like fatty acid synthesis and activation of energy-producing processes such as stimulation of lipid oxidation through the phosphorylation of acetyl-CoA carboxylase, ACC1 and ACC2, resulting in their inactivation<sup>221,222</sup>. In cells undergoing nutritional stress, AMPK regulates a catabolic process called autophagy to maintain the cellular energy levels as well as cell survival<sup>223,224</sup>. Mitophagy is a special class of autophagy where damaged mitochondria are removed in starved cells. AMPK plays an important role in regulation of mitophagy via phosphorylation of the ULK kinases leading to autophagy induction. A feedback loop is activated where ULK kinases via phosphorylation of AMPK subunits may negatively regulate AMPK signaling<sup>224,225</sup>. In situations of chronic nutrient starvation, AMPK can also phosphorylate the transcriptional co-activator PGC1a, transcription factor FOXO3, or the core histone H2B, resulting in regulation of gene transcription<sup>226</sup>. Studies

with AMPK $\alpha$ -deficient cell lines and animal models indicate that AMPK is also involved in regulation of tumor metabolism; however the exact role for AMPK in stimulating glycolysis in cancer cells is still not clearly understood<sup>227</sup>. Additionally, studies show that the expression of Hypoxia Inducible Factor 1 $\alpha$  (HIF-1 $\alpha$ ), a critical player in the Warburg effect is negatively regulated by AMPK<sup>228-230</sup>.

The mammalian target of rapamycin (mTOR) is downstream of AMPK signaling (Figure 2). mTOR exists in two distinct complexes, TORC1 and TORC2, differentiated based on the associated proteins. TORC1 has two direct targets, p70S6K (p70 ribosomal S6 kinase 1) and 4EBP1 (eukaryotic initiation factor 4E binding protein 1), and thus regulates protein synthesis in response to growth factors like insulin-like growth factor<sup>231</sup>. When growth factors bind to their receptors, activation of mTOR signaling takes place resulting in up regulated synthesis of growth regulatory proteins. When the cellular energy level drops due to different types of stress conditions such as nutrient shortage, AMPK gets activated that result in inhibition of mTOR signaling leading to decreased protein synthesis to conserve cellular energy. Studies have shown that AMPK phosphorylates raptor, aTORC1 subunit that in turn plays an important role in the inhibition of mTOR signaling by AMPK. mTORC1 also regulates cell growth and cell fate via autophagy induction<sup>232</sup>. Cancer survival and progression requires synthesis of fatty acids, triglycerides, cholesterol, RNA, and proteins. As all these processes are energy demanding, metabolic stress is induced resulting in AMPK activation ultimately leading to the inhibition of energy consuming processes<sup>233</sup>.

Cell growth is regulated by AMPK through mTORC1 pathway and loss of AMPK promotes uncontrolled up regulation of the mTORC1 signaling resulting in enhanced cell growth and proliferation<sup>232</sup>. AMPK directly phosphorylates TSC2 at serine 1387. TSC2 is a tumor suppressor protein with mTORC1 inhibitory function<sup>234</sup>. Activated AMPK can directly phosphorylate Raptor resulting in 14-3-3-mediated inhibition of mTORC1 signaling<sup>235</sup>. In

addition, a combination of AMPK inhibition and maintaining mTORC1 signaling would increase tumor growth via bypassing these cellular metabolic brakes. Thus AMPK functions as a cellular metabolic tumor suppressor protein, inhibiting cancer cell growth via regulating cellular metabolism and growth promoting pathways<sup>236</sup>. Studies show that under experimental conditions, AMPK also regulates cell polarity and cytoskeletal dynamics<sup>237</sup>.

### **AMPK and Cancer**

AMPK connects diverse networks of tumor suppressors including LKB1, TSC2 and p53<sup>238</sup>. As AMPK plays such an important role in the regulation of cancer cell metabolism, it is no surprising that loss of AMPK activity has been observed in many tumor types and reprogramming of cancer cell metabolism as well as accelerated cell growth and proliferation has been connected to dysregulated AMPK activity<sup>227</sup>. In a preclinical study, loss of AMPK has been shown to enhance Myc-dependent lymphogenesis, indicating that loss of AMPK could be exploited by oncogenic drivers for the promotion of tumorigenesis in mice<sup>239</sup>. When PTEN-deficient mice, whose mTOR signaling is high due to the constitutively activated Akt were crossed with LKB1-deficient mice, tumor developed at a faster rate, even though LKB1-deficient mice did not develop tumors. Tumor onset was delayed when these PTEN-deficient mice were administrated with AMPK activators. Therefore, these observations suggest that AMPK activators might be useful anti-cancer drugs for tumors like breast cancer where mTOR signaling is over activated<sup>227,240</sup>.

Up regulated mTOR signaling has been observed in many cancers<sup>241</sup>. It has been shown that the AMPK phosphorylates the subunit of TORC1 raptor resulting in the inhibition of mTOR signaling. Conversely, AMPK activation could also provide growth advantage to cancer cells by permitting them to adapt to metabolic stress<sup>242</sup>. It should be noted that most of studies

supporting the use of AMPK activators as anti-cancer agents are based on the metabolic stress inducing properties of indirect AMPK-activating compounds.

### **AMPK Activators Overview: Direct and Indirect**

AMPK activators could be divided into two categories, direct and indirect activators. There is a surge of studies for compounds that were suggested to have AMPK-activating properties. However this section only covers AMPK-activating compounds with relatively clear understanding of their mechanisms of action.

#### **Direct AMPK Activators**

##### **5-Aminoimidazole-4-carboxamide-1- $\beta$ -d-ribofuranoside (AICAR) and ZMP**

AICAR is an AMP mimetic compound that could get phosphorylated to ZMP, a structurally similar compound to AMP. As an AMPK agonist, AICAR directly binds to the AMPK- $\gamma$  subunit AMPK, and inhibits proliferation and induces senescence as well as apoptosis *via* activation of AMPK in cancer cells. Previously, AICAR has been tried to minimize the severity of heart attacks, as well to treat metabolic disorders, but currently it is used only as a study tool in AMPK research field<sup>243,244</sup>. AICAR treatment leads to c-Jun N-terminal kinases (JNKs) and caspase-3 activation as well as mTOR pathway inhibition, resulting in apoptosis induction in cancer cells<sup>245</sup>. Additionally, when treated with AICAR, significant inhibition of proliferation with cell cycle arrest in S-phase was observed in cancer cells. The observations that AICAR may inhibit cancer cell growth further support the rationale for targeting AMPK to treat cancer<sup>246</sup>.

#### **Salicylates and A-769662**

Historically, salicylic acid was thought to have medicinal properties and was isolated from willow bark (*Salix Alba*)<sup>247</sup>. It has been shown that plants produce salicylic acid as a

defensive mechanism against infectious pathogens. The term 'salicylates' includes salts as well as esters of salicylic acid, although in the present day, salicylates are replaced by aspirin, its synthetic acetylated derivative for therapeutic purposes<sup>248</sup>. Additionally, self-condensed dimer of salicylic acid, salsalate also possesses therapeutic properties. Interestingly, both aspirin and salsalate are quickly metabolized to salicylic acid *in vivo* following its administration to the patients. Importantly, salicylate can activate AMPK at physiological concentrations achieved following the administration of higher doses of either aspirin or salsalate in patients<sup>249</sup>.

The direct binding of salicylate to AMPK results in its allosteric activation via inhibiting the dephosphorylation of the activation site threonine 172 on the AMPK  $\alpha$  subunit. Similar to the synthetic AMPK activator, A-769662, Salicylate also binds to the AMPK  $\beta$  subunit<sup>250</sup>. In AMPK-knockout mice, the ability of salicylate to increase fat utilization and to decrease plasma levels of fatty acid was attenuated further suggesting that AMPK could be the target for salicylate. It should be noted, however, that cyclooxygenase as well as IKK $\beta$  inhibition might also contribute to the therapeutic properties of aspirin as well as salicylate<sup>251</sup>. Interestingly, in mice deficient with cyclooxygenase and IKK $\beta$ , some of these effects were still observed indicating that salicylate may have additional undetermined, targets<sup>252</sup>. Importantly, a significantly reduced risk for colorectal cancer and other adenocarcinomas was observed in patients taking daily aspirin for 5 or more years<sup>253,254</sup>. Also, lower risk for prostate cancer has been observed in men taking aspirin every day<sup>255</sup>. Various *in vitro* and *in vivo* preclinical studies suggest that AMPK-activating ability of aspirin could be at least partially responsible for its chemopreventive properties<sup>256,257</sup>.

### Indirect AMPK Activators

Although very few direct activators of AMPK have been reported, most of compounds activate AMPK via an indirect mechanism such as activation of metabolic stress or targeting an

upstream regulator of AMPK signaling.

### **Biguanides: Metformin and Phenformin**

Metformin and phenformin belong to the 'biguanide' class of antidiabetic agents. Dubbed as most frequently prescribed Type II diabetes medication, they can activate AMPK via its upstream kinase, LKB1 and inhibition of complex I of the mitochondrial respiratory chain<sup>258</sup>. Various clinical studies are currently investigating their chemopreventive properties in colorectal, prostate and breast cancer<sup>259-262</sup>. It has been shown that AMPK activation by metformin triggers a growth inhibitory signal via a transcription-independent induction of BCA2, an E3 ligase with a corresponding enhanced activation of AKT signaling. Additionally, BCA2 knockdown as well as pharmacological inhibition of AKT signaling enhanced growth inhibitory properties of metformin in human breast cancer cells suggesting that combination of metformin with a BCA2 inhibitor could be used for breast cancer treatment<sup>263</sup>. Interestingly, it has been shown that metformin at low concentrations such as 60-80 $\mu$ M inhibits glucose production as well as gluconeogenic gene expression in the primary hepatocytes through AMPK-dependent mechanism suggesting that metformin could directly activate AMPK<sup>264</sup>. Further in depth studies are needed to confirm the exact mechanism of AMPK activation due to metformin.

### **Natural AMPK Activators**

Beside above mentioned AMPK activators, continuously expanding group of diverse natural products or dietary compounds have been found to possess AMPK-activating potential. These include resveratrol, epigallocatechin-3-gallate (EGCG), obovatol, cucurbitacins, ginsenosides, and glabridin. The exact AMPK-activating mechanisms for these compounds are still not very clear but studies show that most of these compounds act as indirect AMPK activators<sup>265</sup>.

### **AMPK: Concluding Remarks**

Myriad studies have emerged during last few years suggesting an anticancer role for AMPK. It poses as a viable therapeutic target with a possibility that AMPK activators could be used as chemopreventive or anticancer agents. Several preclinical studies have shown that metformin and phenformin delayed tumor progression in tumor xenograft models. Additional evidences suggesting use of AMPK activators as anticancer strategy came from studies with AICAR and salicylate where these compounds inhibited cancer cell proliferation in cell culture and animal models as well as cancer patients. Retrospective epidemiological studies show that patients who take metformin or aspirin have less probability of getting cancer. However, the exact mechanism of aspirin's anticancer properties is still not clear and needs further in depth preclinical as well as clinical studies<sup>265</sup>. Several new studies are reporting AMPK-activating capabilities of drugs that are used for the treatment of wide range of diseases. Originating from the observation that different classes of proteasome inhibitors activate AMPK in breast as well as other cancer cell lines, I studied the mechanism of the AMPK activation by proteasome inhibitors in cancer cells.

## CHAPTER 2

### MATERIALS AND METHODS

#### Materials

3-(4,5-Dimethylthiazol-2-yl)-2,5-diphenyltetrazolium bromide (MTT), dimethyl sulfoxide (DMSO), verapamil hydrochloride, and nifedipine hydrochloride were obtained from Sigma–Aldrich (St. Louis, MO, USA). MG132 and bortezomib were obtained from Boston Biochem (Cambridge, MA), LC Laboratories (Woburn, MA). Carfilzomib was obtained from Investigational Pharmacy at Karmanos Cancer Center. DMEM/F12 (1:1), penicillin, and streptomycin were purchased from Invitrogen (Carlsbad, CA). Fetal bovine serum was purchased from Aleken biological (Nash, TX). Purified human 20S proteasome and Suc-LLVY-AMC, the fluorogenic peptide substrate for the proteasomal CT like activity, were obtained from Calbiochem (San Diego, CA, USA). CellEvent Caspase 3/7 green detection reagent was obtained from Invitrogen. Mouse monoclonal antibody against human poly(ADP-ribose) polymerase (PARP) was purchased from BioMol International LP (Plymouth Meeting, PA). Mouse monoclonal antibody against ubiquitin (P4D1), mouse monoclonal antibody against p27<sup>kip1</sup>, rabbit polyclonal antibody against IκBα (C-15), goat polyclonal antibody against β-actin (C-11), and secondary antibodies were purchased from Santa Cruz Biotechnology, Inc. (Santa Cruz, CA).

#### Cell culture and cell extract preparation

Human breast cancer MDA-MB-231 and MDA-MB-468 cells were grown in DMEM/F-12 media supplemented with 10% (v/v) fetal bovine serum, 100 units/mL of penicillin, and 100 µg/mL of streptomycin. Human lung cancer A549 cells were cultured in RPMI media supplemented with 10% (v/v) fetal bovine serum, 100 units/ml of penicillin, and 100 µg/ml of streptomycin. Human cervical cancer HeLa cells were grown in DMEM high glucose medium



supplemented with 10% fetal bovine serum, 100 units/mL of penicillin, 100 µg/mL of streptomycin. All cells were grown in a humidified incubator with an atmosphere of 5% CO<sub>2</sub> and at 37°C.

Whole cell extracts were prepared as follows: MDA-MB-231, MDA-MB-468, A549, and HeLa cells were grown to 70-80% confluency, treated under various conditions, harvested, washed with 1X PBS, and homogenized in a lysis buffer [50 mM Tris-HCl (pH 8.0), 150 mM NaCl, 0.5% NP40 (v/v)] for 20 min at 4°C. Afterwards, the lysates were centrifuged at 12,000 g for 12 minutes and the supernatants were collected as whole cell extracts.

### **Cell proliferation assay**

5000 cells / 100 µl of cell culture media were plated in a 96 well plate and grown until they were 70-80% confluent, followed by the treatment with either vehicle control or various concentrations of test compounds as indicated in the figure legends for 48 hours. Percent relative cell proliferation was measured by 3-(4,5-Dimethylthiazol-2-yl)-2,5-diphenyltetrazolium bromide (MTT) assay as described previously<sup>266</sup>.

### **Proteasomal activity assay using whole cell extracts**

MDA-MB-231 cells were grown to 70-80% confluency and treated as indicated in the figure legends, harvested, and used for whole cell extract preparation. Cell extracts after each treatment were incubated at 37°C for 2 hours with the fluorogenic substrate Suc-LLVY-AMC and production of hydrolyzed AMC groups was measured with the Wallac Victor<sup>3</sup> multilabel counter with an excitation filter of 365 nm and emission filter of 460 nm. In another experiment, cell extracts from untreated MDA-MB-231 cells were incubated with indicated concentrations of verapamil for an hour at 37°C in an incubator. The fluorogenic substrate Suc-LLVY-AMC (for the proteasomal chymotrypsin) was added to the mixture and incubated for additional 2 hours at

37°C. Production of hydrolyzed AMC groups was measured with the Wallac Victor<sup>3</sup> multilabel counter with an excitation filter of 365 nm and emission filter of 460 nm.

### **Analysis of chymotrypsin like proteasomal activity using whole cell extracts from treated cells**

MDA-MB-231, MDA-MB-468, A549 and HeLa cells were grown to 70-80% confluency, treated under various conditions, harvested, and used for whole cell extract preparation as described earlier. Whole cell extract (7.5 µg) was incubated with the fluorogenic peptide substrate Suc-LLVY-AMC, specific for the proteasomal CT-like activity (20 µM), in 100 µL assay buffer [20 mmol/L Tris-HCl (pH 7.5)]. After 1-2 hours incubation at 37°C, inhibition of CT-like proteasomal activity was measured using a Victor 3 Multilabel Counter with an excitation filter of 380 nm and an emission filter of 460 nm (PerkinElmer, Boston, MA, USA). Changes in fluorescence were calculated against solvent-treated controls and plotted using Microsoft Excel™ software.

### **Purified 20S proteasome activity assay**

Purified human 20S proteasome (35 ng) was incubated in 100 µl of assay buffer (50mmol/L Tris-HCl, pH 7.5) with indicated concentrations of verapamil for an hour at 37°C in an incubator. The fluorogenic substrate Suc-LLVY-AMC (for the proteasomal chymotrypsin like activity) was added to the mixture and incubated for additional 2 hours at 37°C. Production of hydrolyzed AMC groups was measured with the Wallac Victor<sup>3</sup> multilabel counter with an excitation filter of 365 nm and emission filter of 460 nm.

### **Cellular morphology analysis**

Cancer cells were plated and allowed to grow overnight, followed by indicated treatments. The morphological changes in the cells were observed using a Zeiss (Thornwood, NY) Axiovert 25 microscope with phase contrast.

### **Caspase-3/7 detection**

CellEvent Caspase-3/7 green detection reagent (Invitrogen) was used to detect apoptotic cells. Briefly, cells were plated, allowed to grow overnight followed by indicated treatments for 24 hours. CellEvent Caspase-3/7 green detection reagent was added to the plates and images were taken with fluorescence microscope.

### **siRNA mediated knockdown**

The custom designed small interfering RNA (*siRNA*) duplexes for CaMKK $\beta$  (Santa cruz biotechnology, sc-38955) and non-silencing scrambled *siRNA* negative control (Qiagen, S103650318) were used for the transfection of MDA-MB-468 cells. Cells were plated in 6 well plates and, when reached 80% confluency, were transfected with either control or specific *siRNA* to CaMKK $\beta$ , as per manufacturers protocol using Hiperfect transfection reagent for 60 hours, after which cells were treated with either vehicle or bortezomib for indicated hours in the legends, and samples were harvested, lysed and analyzed by Western blotting.

### **Western blot analysis**

MDA-MB-231, MDA-MB-468, A549, and HeLa cells were grown to 70-80% confluency, treated under various conditions, harvested, and used for whole cell extract preparation as described earlier. Cell lysates were prepared by boiling the samples with equal amounts of 2X sodium dodecyl sulfate (SDS) buffer for 5 minutes at 100°C. Cell lysates (30 $\mu$ g of proteins per

lane) were separated by SDS-Polyacrylamide gel electrophoresis (PAGE) and transferred to a nitrocellulose membrane, followed by blocking in 5% milk-TBS-TWEEN (TBST) solution and incubated with specific primary antibodies for at least 24 hours at 4 °C. After washing with TBST solution, followed by incubation with respective secondary antibodies and washing with TBST, visualization was done using the HyGLO chemiluminescent HRP.

### **CaMKK $\beta$ RNA analysis by qPCR**

Total RNA was isolated from MDA-MB-468 cells using RNeasy Mini Kit (Qiagen, Georgetown, MD) according to manufacturer's protocol and was reverse transcribed to complementary DNA using Superscript VILO cDNA synthesis Kit (Qiagen, Georgetown, MD), according to the vendor's instructions. Primers for CaMKK $\beta$  (4331182, Hs00198032\_m1) and GAPDH (4331182, Hs02758991\_g1) were obtained from life technologies (Carlsbad, CA). cDNA was measured by quantitative real-time PCR using Applied Biosystems StepOnePlus Real Time PCR Systems (Life Technologies, Carlsbad, CA) and TaqMan Gene Expression Master Mix (Life Technologies, Carlsbad, CA).  $C_T$  values were normalized to those of GAPDH.

### **Image J analysis**

Image J analysis software (NIH) was used to perform Western blot densitometry analysis. Phosphorylated AMPK was normalized to corresponding total AMPK where as CaMKK $\beta$  was normalized to  $\beta$ -actin. Fold Change was calculated based on the vehicle control lane.

### **Statistical Analysis**

Statistical analyses were carried out with the R software package (Version 3.1.3) and were based on the parametric one-way ANOVA. The pairwise post-hoc t-test was applied and then adjusted by Holm's method for errors of multiplicity. The nonparametric one-way ANOVA

using Kruskal-Wallis test, followed by Wilcoxon pairwise post-hoc procedures using Holm's method, was also applied as a reference. In general, the results of nonparametric methods were consistent with those of parametric methods. Boxplot illustrations were used to depict the median values and interquartile ranges of percentage relative cell proliferation and were given without outliers and extreme values. *P* values of <0.05 were considered significant.

### CHAPTER 3

#### **Proteasome inhibitors induce AMPK activation via CaMKK $\beta$ in human breast cancer cells**

*Adapted from manuscript published in Breast Cancer Research and Treatments, 2015, July 31*

*[Epub ahead of print]*

AMPK and Ubiquitin Proteasome System (UPS) have gained great attention as therapeutic targets for the treatment of certain types of cancers. While AMPK serves as a master regulator of cellular metabolism, UPS regulates protein homeostasis. Some studies have suggested that they crosstalk although the exact mechanism is not very clear. AMPK activation by a proteasome inhibitor might affect its own anticancer properties. Therefore, it is important to explore the link between AMPK activation by proteasome inhibitors towards the development of novel therapies for treating breast cancer.

## RESULTS

### Different proteasome inhibitors activate AMPK in MDA-MB-231 cells

Based on their chemical structures, MG132, bortezomib, and carfilzomib are divided into different classes of proteasome inhibitors. Additionally, MG132 and bortezomib are reversible proteasome inhibitors whereas carfilzomib is an irreversible proteasome inhibitor<sup>50</sup>. Owing to high toxicities and short half-life, MG132 was not approved for clinical use whereas bortezomib and carfilzomib are approved for the treatment of Multiple Myeloma<sup>50</sup>. When human breast cancer MDA-MB-231 cells were treated with 200 nM MG132, 10 nM bortezomib or 10 nM carfilzomib for up to 24 h, AMPK was phosphorylated at threonine 172 (up to 6-folds) while there was relatively less change in the levels of total AMPK protein (Figure 3A-C), indicating AMPK activation. Also, accumulation of ubiquitinated proteins (Figure 3) and decreased proteasomal chymotrypsin-like activity in the treated cells confirm proteasome inhibition. These results provide evidence that AMPK activation could be induced by various proteasome inhibitors which does not depend on their structures or modes of binding to the proteasome.

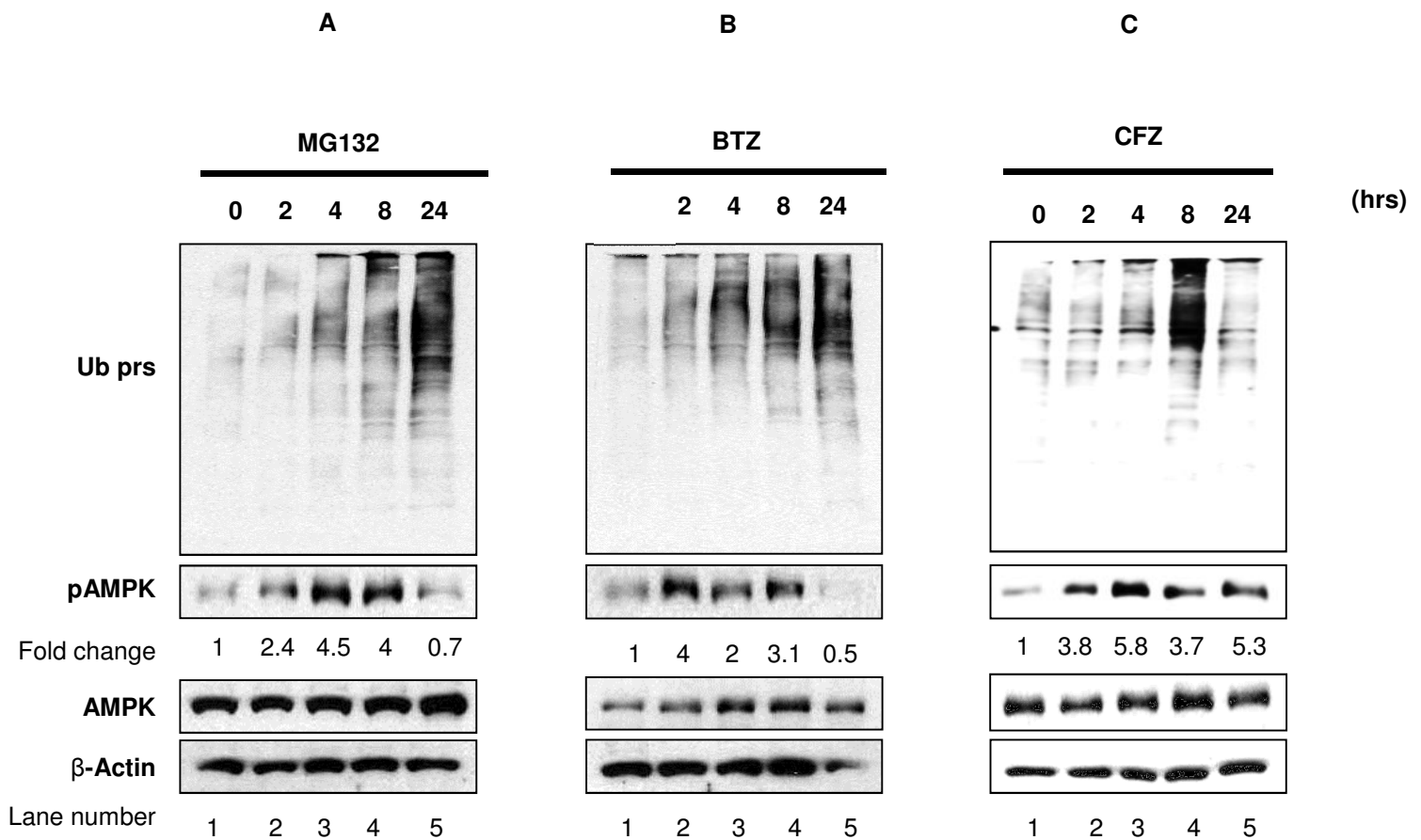


**Figure 3: Proteasome inhibitors induce AMPK activation in MDA-MB-231 cells**

MDA-MB-231 breast cancer cells were treated with DMSO or 200 nM MG132 (A), 10 nM bortezomib (B) or 10 nM carfilzomib (C) for up to 24 hours. Cell extracts were used for Western blot analysis with specific antibodies for pAMPK, AMPK, ubiquitin and  $\beta$ -actin. The data showed in Figure 3A is a representative of two independent experiments. The data showed in Figure 3B is representative of four independent experiments. The data showed in Figure 3C is a representative of two independent experiments. Fold increase in pAMPK/AMPK ratio was calculated based on densitometry for the specific blots presented here.



## **CaMKK $\beta$ regulates proteasome inhibition-mediated AMPK activation in MDA-MB-468 cells**

We then investigated the upstream kinase(s), such as CaMKK $\beta$  or LKB1 for AMPK activation by proteasome inhibitors. We first employed a selective, cell permeable, pharmacological inhibitor, STO-609 for CaMKK $\beta$ <sup>214</sup>. Human breast cancer MDA-MB-468 cells were treated with carfilzomib and STO-609 or each agent alone, followed by measurement of AMPK phosphorylation. We observed that use of STO-609 diminished carfilzomib-induced AMPK activation in co-treated MDA-MB-468 cells (Figure 4A). We observed similar inhibition of AMPK activation when MDA-MB-468 cells were treated with combination of bortezomib and STO-609, as compared to each agent alone (Figure 4C). Interestingly, carfilzomib or bortezomib co-treatment with STO-609 for 4 and 8 hours also attenuated the accumulation of ubiquitinated proteins when compared to the proteasome inhibitor alone (Figure 4A and C). These results suggest the involvement of CaMKK $\beta$  as the upstream kinase in AMPK activation by proteasome inhibitors. These results also demonstrate that proteasome inhibition-induced AMPK activation is not limited to a single breast cancer cell line.

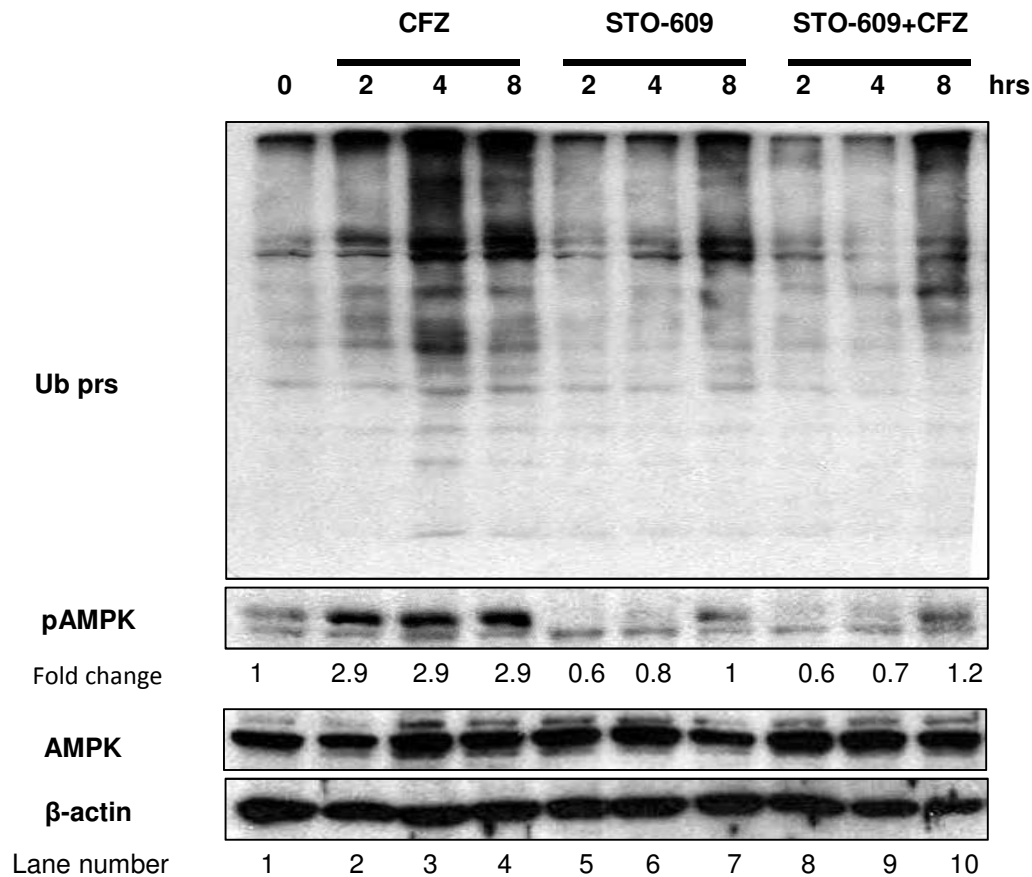


**Figure 4A: Effect of CaMKK $\beta$  inhibition on AMPK activation by proteasome inhibitor, carfilzomib in MDA-MB-468 cells**

MDA-MB-468 breast cancer cells were treated with either 10 nM carfilzomib with or without 10  $\mu$ M STO-609 for up to 8 hours. Cell extracts were used for Western blotting with specific antibodies for pAMPK, AMPK, ubiquitin and  $\beta$ -actin. The data showed in Figure 4A is a representative of two independent experiments. Fold increase in pAMPK/AMPK ratio was calculated based on densitometry for the specific blots presented here.

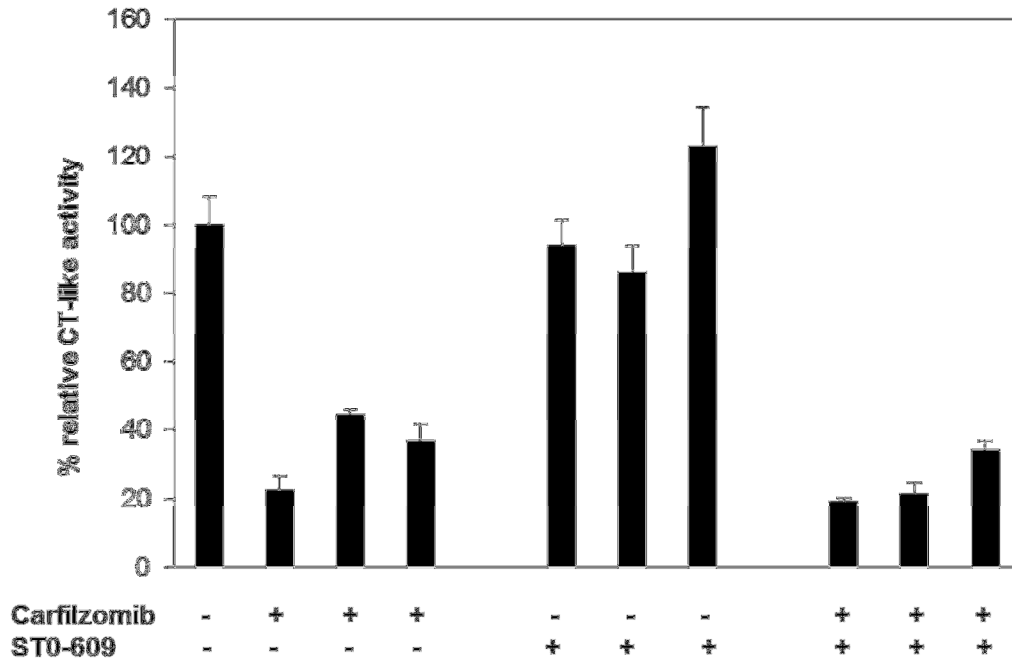


**Figure 4B: Effects of carfilzomib and STO-609 in MDA-MB-468 cells**

MDA-MB-468 breast cancer cells were treated with either 10 nM carfilzomib with or without 10  $\mu$ M STO-609 for up to 8 hours. Cell extracts were used for the determination of CT-like activities. Measurements of CT-like activity for individual treatment of carfilzomib and STO-609 were performed twice whereas the CT-like activity assay for the combination of carfilzomib and STO-609 was performed once. Each individual experiment was tested in triplicates and the error bars represent the standard deviation.

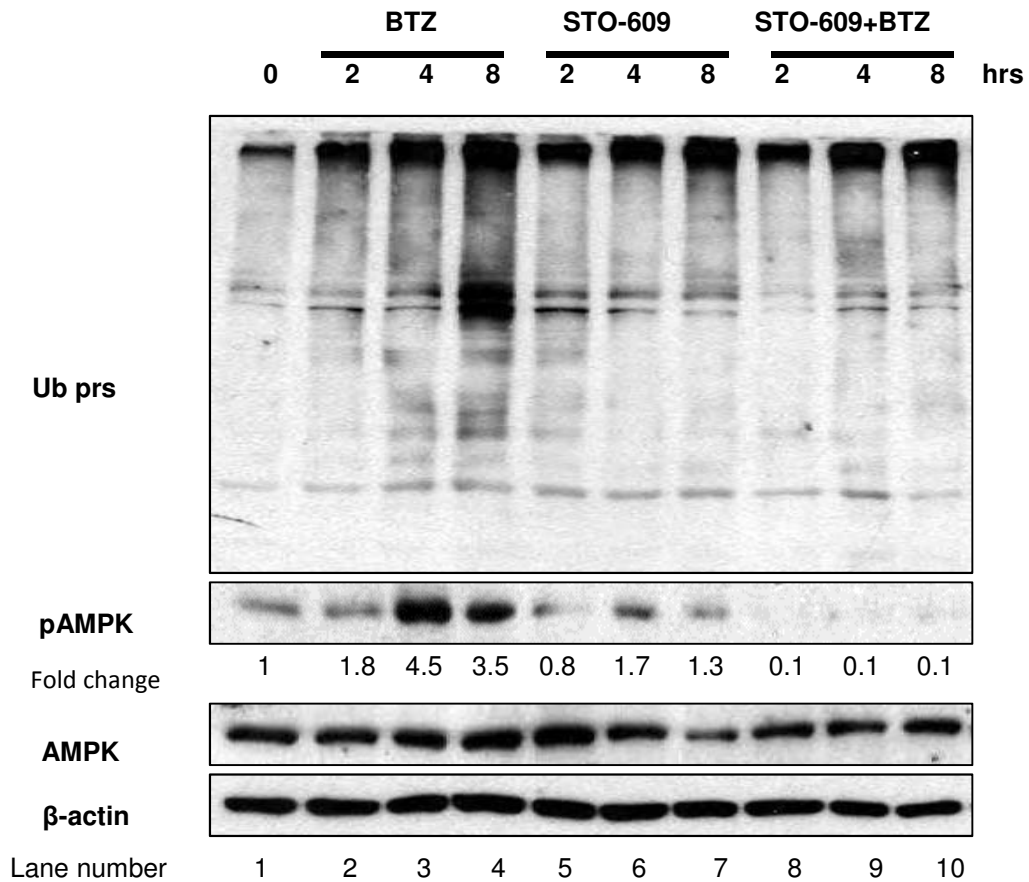


**Figure 4C: Effect of CaMKK $\beta$  inhibition on AMPK activation by proteasome inhibitor, bortezomib in MDA-MB-468 cells**

MDA-MB-468 breast cancer cells were treated with either 10 nM bortezomib with or without 10  $\mu$ M STO-609 for up to 8 hours. Cell extracts were used for Western blotting with specific antibodies for pAMPK, AMPK, ubiquitin and  $\beta$ -actin. The data showed in Figure 4C is a representative of two independent experiments. Fold increase in pAMPK/AMPK ratio was calculated based on densitometry for the specific blots presented here.

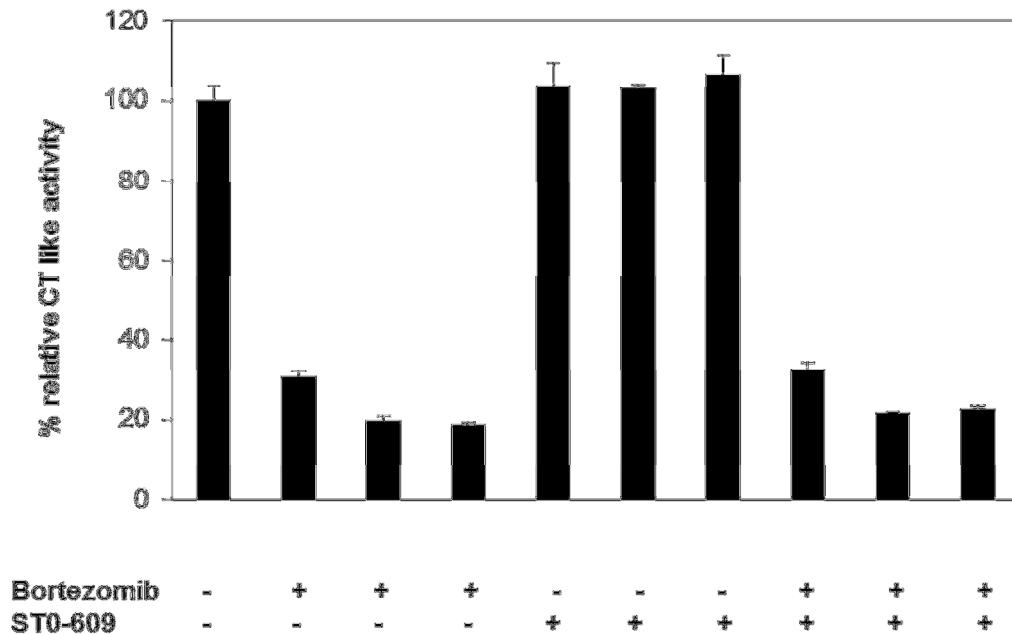


**Figure 4D: Effects of bortezomib and STO-609 in MDA-MB-468 cells**

MDA-MB-468 breast cancer cells were treated with either 10 nM carfilzomib with or without 10  $\mu$ M STO-609 for up to 8 hours. Cell extracts were used for the determination of CT-like activities. Error bars correspond to standard deviation in triplicates for each experimental condition. The measurements of CT-like activity for bortezomib alone treatment were performed four times. The measurement of CT-like activity for STO-609 was performed twice. The measurement of CT-like activity for the combination of bortezomib and STO-609 was done once. Each individual experiment was tested in triplicates and the error bars represent the standard deviation.

### **Activation of AMPK by bortezomib in human cancer cells lacking functional LKB1**

It has been shown that LKB1 could serve as an AMPK activator in variety of cells under different conditions<sup>267</sup>. We therefore investigated the possible involvement of LKB1 in AMPK activation by proteasome inhibitors by using A549 and HeLa cells that have either nonfunctional or null LKB1<sup>268,269</sup>, respectively. These cells were treated with bortezomib, STO-609 or their combination. Again, increased levels of phosphorylated/active AMPK, but not total AMPK protein were observed when these cells were treated with bortezomib alone, which was inhibited completely after co-treatment with the selective CaMKK $\beta$  inhibitor STO-609 (Figure 5A and C), further supporting the role of CaMMK $\beta$  in proteasome inhibitor-induced AMPK activation. We also observed little inhibition on accumulation of ubiquitinated proteins by these proteasome inhibitors under the used experimental conditions (Figure 5A and C).

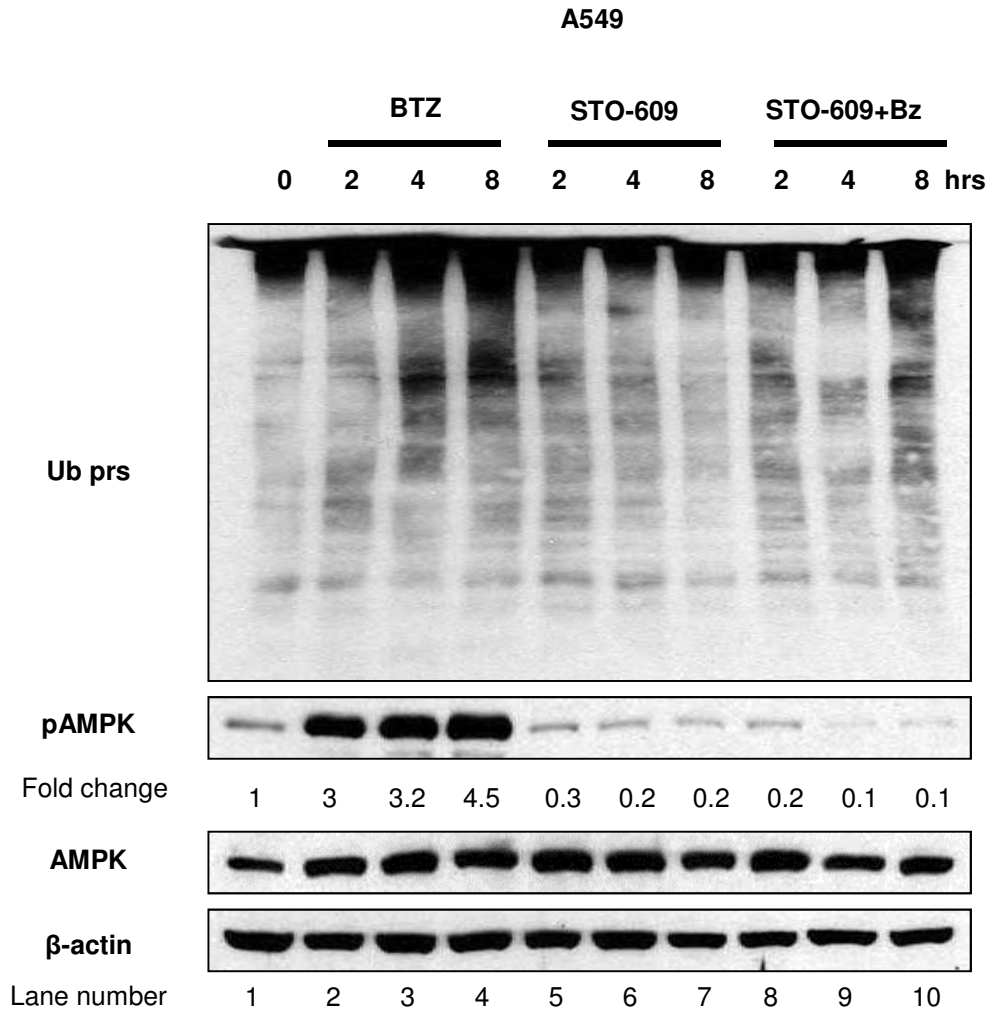


**Figure 5A: CaMKK $\beta$  inhibition decreases AMPK activation in LKB1-dysfunctional A549 lung cancer cells**

A549 lung cancer cells were treated with 10 nM bortezomib with or without 10  $\mu$ M STO-609 for up to 8 hours. Cell extracts were used for Western blotting with specific antibodies for pAMPK, AMPK, ubiquitin, and  $\beta$ -actin. The data showed in Figure 5A is a representative of two independent experiments. Fold increase in pAMPK/AMPK ratio was calculated based on densitometry for the specific blots presented here.

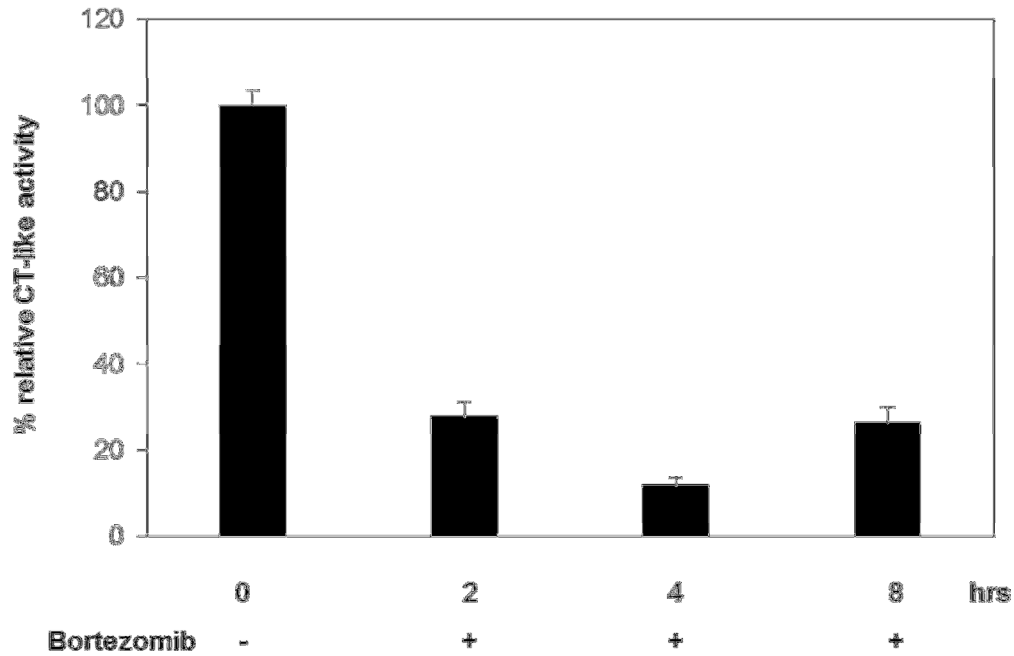


**Figure 5B: Proteasome inhibitory activities of bortezomib in LKB1-dysfunctional A549 lung cancer cells**

MDA-MB-468 breast cancer cells were treated with either 10 nM bortezomib for up to 24 hours. Cell extracts were used for the determination of CT-like activities. Measurements of CT-like activity for the treatment of bortezomib alone in A549 cells were performed twice. Each individual experiment was tested in triplicates and the error bars represent the standard deviation.



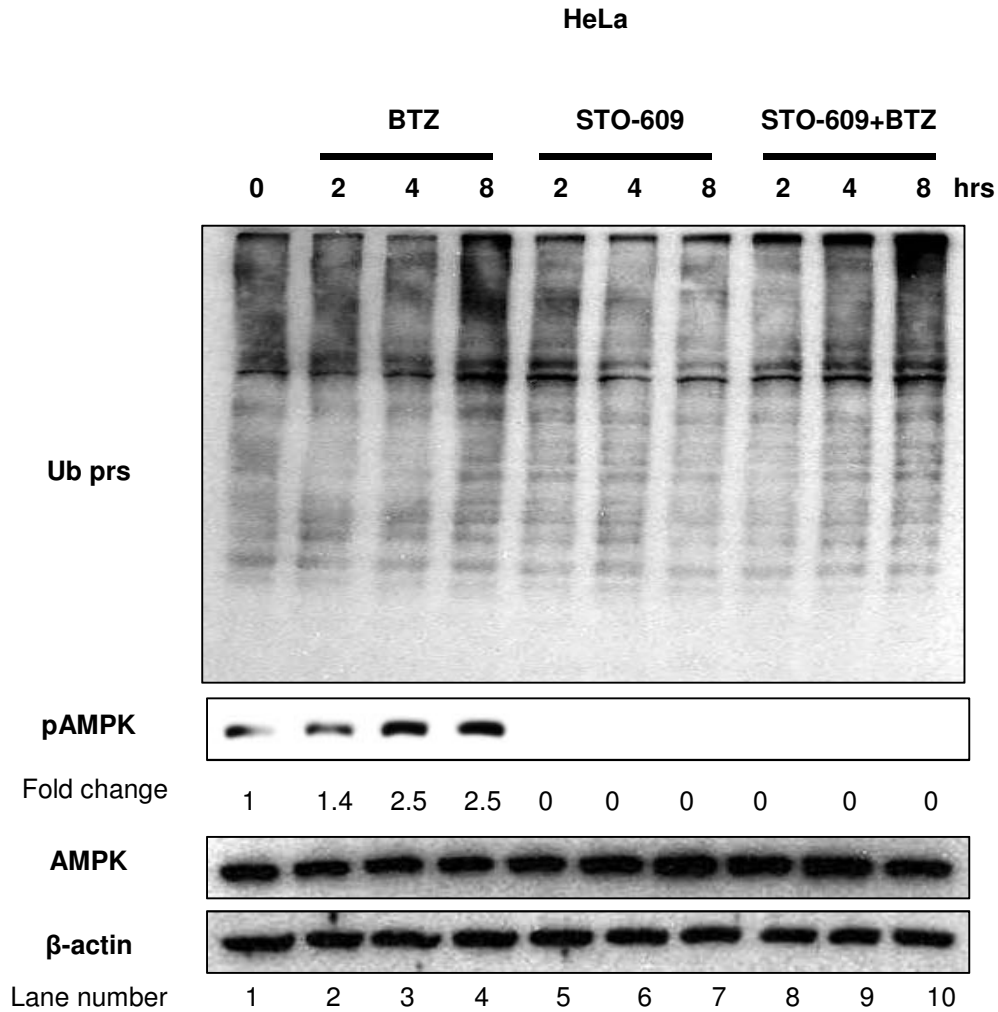


**Figure 5C: CaMKK $\beta$  inhibition decreases AMPK activation in LKB1-deficient HeLa cervical cancer cells**

HeLa cervical cancer cells were treated with 10 nM bortezomib with or without 10  $\mu$ M STO-609 for up to 8 hours. Cell extracts were used for Western blotting with specific antibodies for pAMPK, AMPK, ubiquitin, and  $\beta$ -actin. The data showed in Figure 5C is a representative of two independent experiments. Fold increase in pAMPK/AMPK ratio was calculated based on densitometry for the specific blots presented here.

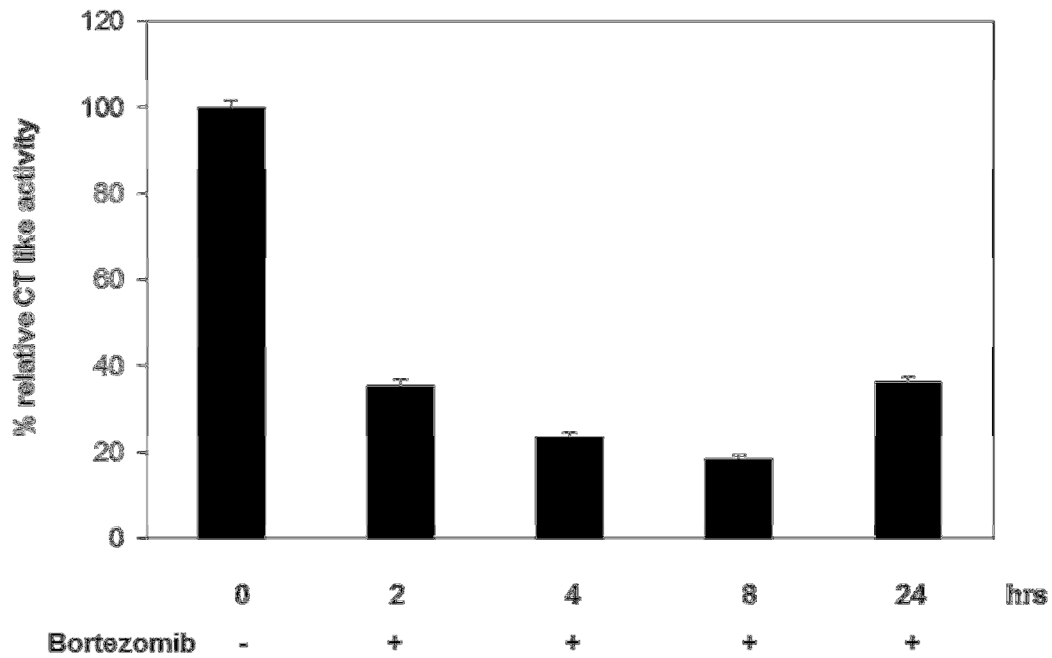


**Figure 5D: Proteasome inhibitory activities of bortezomib in LKB1 deficient HeLa cervical cancer cells**

MDA-MB-468 breast cancer cells were treated with either 10 nM bortezomib for up to 24 hours. Cell extracts were used for the determination of CT-like activities. Measurements of CT-like activity for the treatment of bortezomib alone in HeLa cells were performed twice. Each individual experiment was tested in triplicates and the error bars represent the standard deviation.

### **Ca<sup>2+</sup> regulates bortezomib-induced AMPK activation**

In a majority of the cases, CaMKK $\beta$  is activated by Ca<sup>+2</sup>/calmodulin-dependent mechanisms<sup>214,269,270</sup>. Given that different stimuli may activate different upstream AMPK kinases, we decided to chelate Ca<sup>+2</sup> ions to explore the possibility that elevation of the intracellular calcium levels (resulting from bortezomib treatment) subsequently leads to AMPK activation. We employed BAPTA-AM as an intracellular calcium chelator. BAPTA-AM is an esterified form of Ethylene Glycol Tetraacetic Acid (EGTA) which, upon entering cells, gets de-esterified and becomes an active calcium chelator<sup>271,272</sup>. Our results indicate that intracellular calcium chelation by BAPTA-AM inhibited increased levels of phosphorylated/active AMPK (but not total AMPK protein) and ubiquitinated proteins caused by bortezomib treatment (Figure 6A). Therefore, it is possible the stress resulting from proteasome inhibition could cause opening of calcium channels. To test this possibility, we used extracellular calcium chelator, EGTA, to inhibit the entry of calcium ions into the cells<sup>273</sup>. We found that extracellular calcium chelation by EGTA also led to decreased AMPK activation (Figure 6C). Additionally, bortezomib co-treatment with EGTA for 4 and 8 hours reduced the accumulation of ubiquitinated proteins when compared to bortezomib treatment alone (Figure 6C). Although various studies have reported increases in intracellular calcium levels due to proteasome inhibition, the exact source and mechanism of calcium release is still unknown<sup>274,275</sup>. Our results indicate that both intra and extra-cellular calcium chelators could diminish AMPK activation by bortezomib in human breast cancer cells.

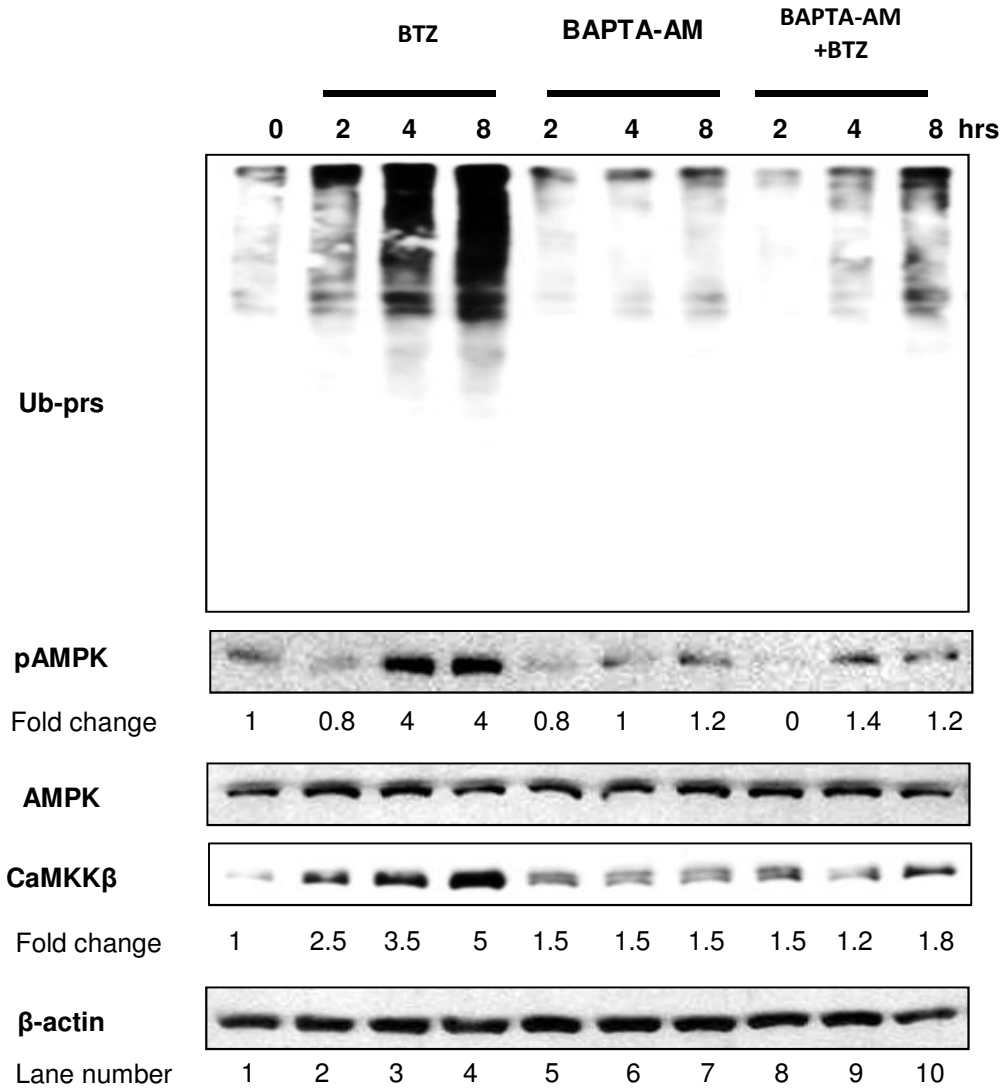


**Figure 6A: Intracellular calcium chelation inhibits bortezomib-induced AMPK activation**

MDA-MB-468 breast cancer cells were treated with 10-nM bortezomib with or without BAPTA-AM for up to 8 hours. Cell extracts were used for Western blotting with specific antibodies for pAMPK, AMPK, CaMKK $\beta$ , ubiquitin, and  $\beta$ -actin. The data showed in Figure 6A is a representative of two independent experiments. Fold increase in pAMPK/AMPK and CaMKK $\beta$ /  $\beta$ -actin ratio was calculated based on densitometry for the specific blots presented here.

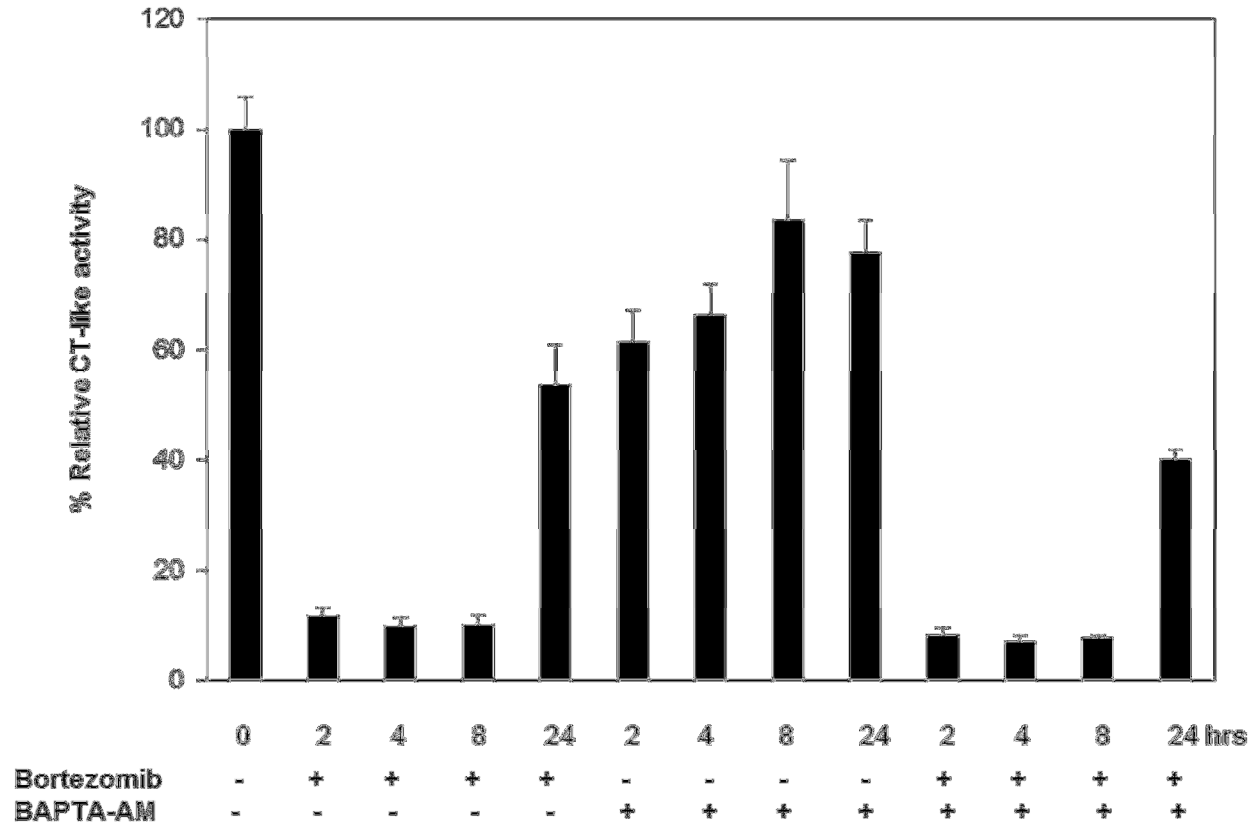


**Figure 6B: Effects of bortezomib and BAPTA-AM in MDA-MB-468 cells**

MDA-MB-468 breast cancer cells were treated with either 10 nM bortezomib with or without BAPTA-AM for up to 24 hours. Cell extracts were used for the determination of CT-like activities. The measurements of CT-like activity for the individual treatment of bortezomib were performed four times. The measurements of CT-like activity for BAPTA-AM as well as for the combination of bortezomib and BAPTA-AM were performed once. Each individual experiment was tested in triplicates and the error bars represent the standard deviation.

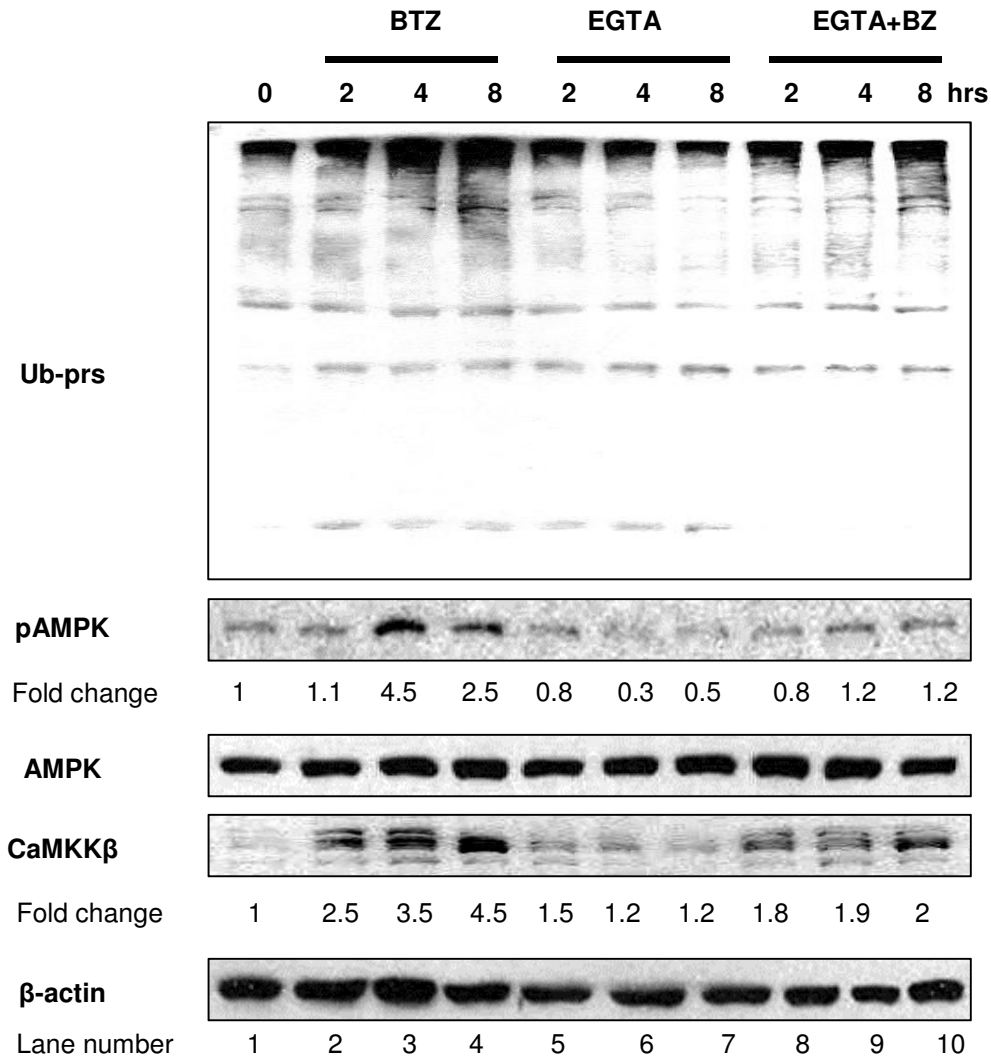


**Figure 6C: Extracellular Calcium chelation inhibits bortezomib-induced AMPK activation**

MDA-MB-468 breast cancer cells were treated with 10-nM bortezomib with or without EGTA for up to 8 hours. Cell extracts were used for Western blotting with specific antibodies for pAMPK, AMPK, CaMKK $\beta$ , ubiquitin and  $\beta$ -actin. The data showed in Figure 6C is a representative of two independent experiments. Fold increase in pAMPK/AMPK and CaMKK $\beta$ /  $\beta$ -actin ratio was calculated based on densitometry for the specific blots presented here.

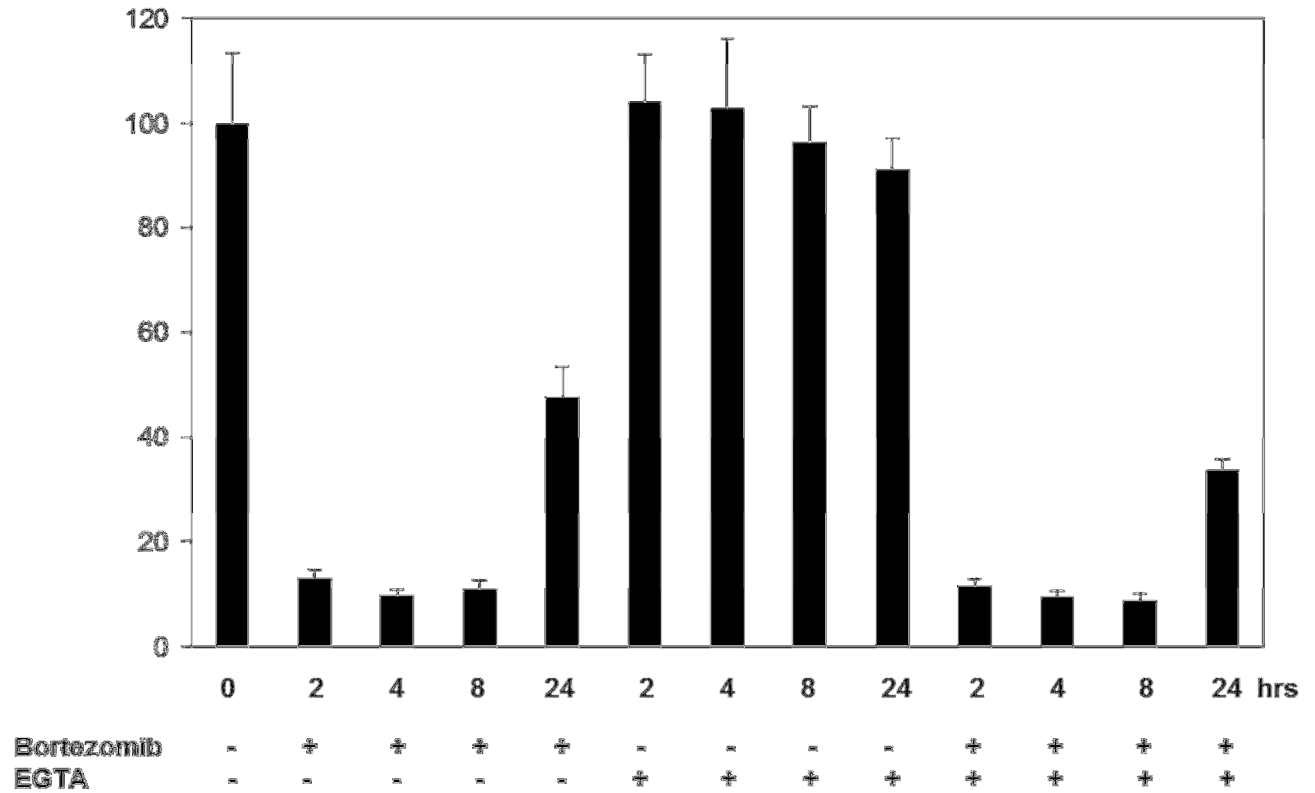


**Figure 6D: Effects of bortezomib and EGTA in MDA-MB-468 cells**

MDA-MB-468 breast cancer cells were treated with either 10 nM bortezomib with or without BAPTA-AM for up to 24 hours. Cell extracts were used for the determination of CT-like activities. Measurements of CT-like activity for the individual treatment of bortezomib were performed four times. The measurements of CT-like activity for EGTA as well as for the combination of bortezomib and EGTA were performed once. Each individual experiment was tested in triplicates and the error bars represent the standard deviation.

### **CaMKK $\beta$ inhibition by siRNA reduces bortezomib-induced AMPK activation**

We observed enhanced accumulation of CaMKK $\beta$  protein in bortezomib-treated cells (Figure 6A and 6C, lanes 1-4). To further confirm the role of CaMKK $\beta$  in AMPK activation by proteasome inhibitors, we used isoform-specific siRNA for CaMKK $\beta$  to inhibit its expression in bortezomib-treated MDA-MB-468 breast cancer cells. We discovered that MDA-MB-468 cells treated with CaMKK $\beta$  siRNA inhibited expression of bortezomib-induced CaMKK $\beta$  protein (indicated in Figure 7, lanes 5-8 vs. 1-4); in addition, MDA-MB-468 cells with CaMKK $\beta$  knockdown, after treatment with bortezomib, failed to increase levels of phosphorylated/active AMPK (Figure 7, lanes 5-8 vs. 1-4). In comparison, siRNA inhibition to CaMKK $\beta$  had little or no effect on levels of total AMPK $\alpha$  protein (Figure 7). Furthermore, CaMKK $\beta$  inhibition by its specific siRNA also partially suppressed accumulation of ubiquitination proteins by bortezomib (Figure 7). The non-silencing scrambled siRNA served as a negative control in this experiment (Figure 7).



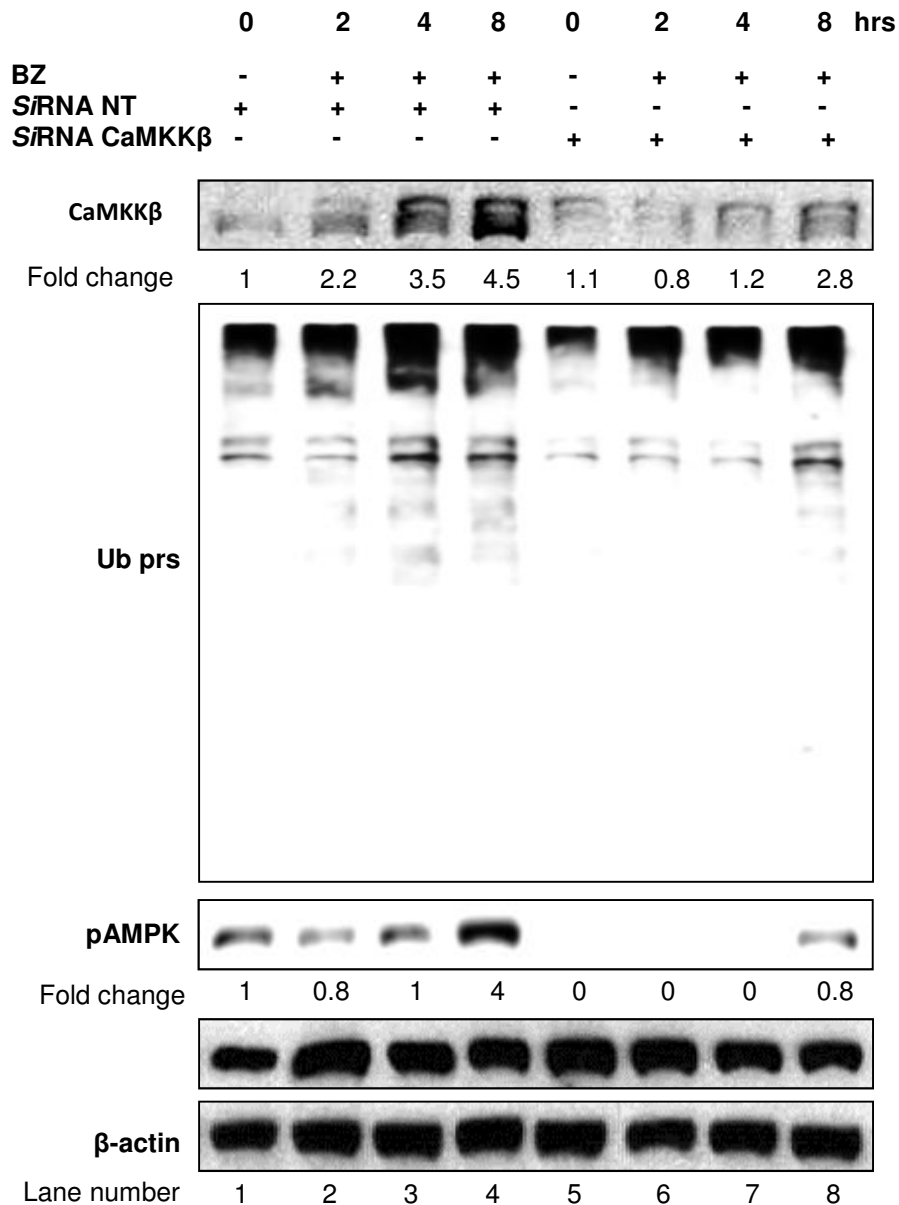


**Figure 7A: CaMKK $\beta$  knockdown decreases AMPK activation induced by bortezomib**

MDA-MB-468 cells, grown in a 6-well plate, were transiently transfected with either 10 nM CaMKK $\beta$  siRNA or scrambled non-silencing siRNA for 60 hours, followed by treatment with 10 nM bortezomib for up to 8 hours. Untreated cells were used as controls. Cell extracts were used for Western blots with specific antibodies for pAMPK, AMPK, CaMKK $\beta$ , ubiquitin, and  $\beta$ -actin. The data showed in Figure 7A is a representative of three independent experiments. Fold increase in pAMPK/AMPK and CaMKK $\beta$ / $\beta$ -actin ratio was calculated based on densitometry for the specific blots presented here.

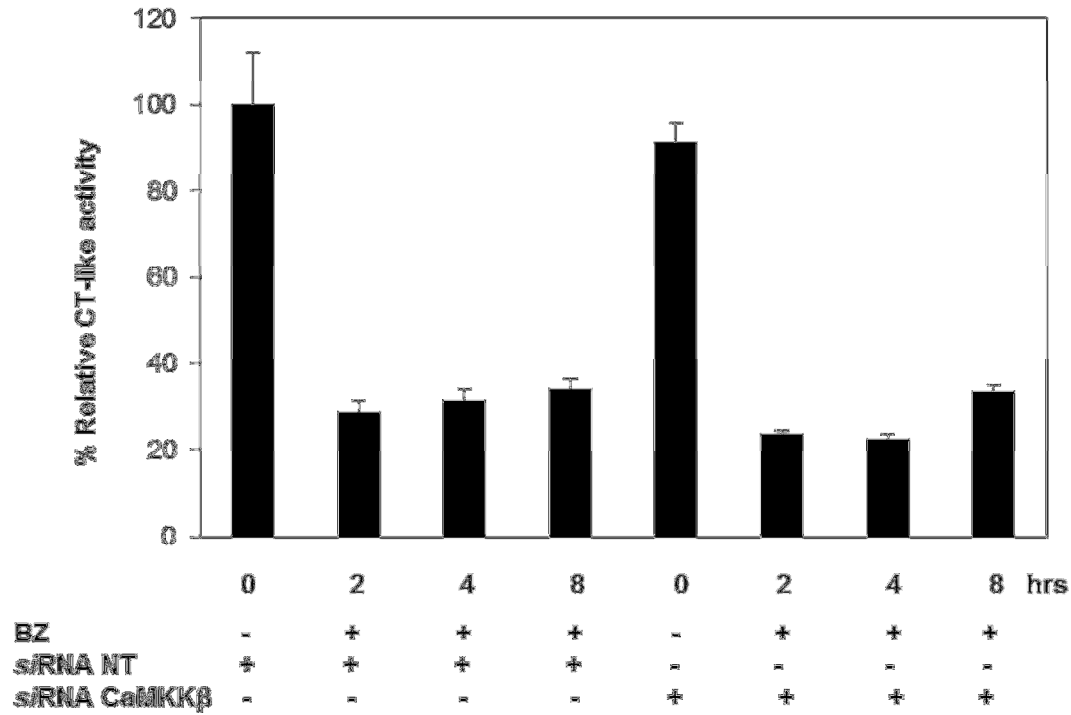


**Figure 7B: Proteasome inhibitory activities of bortezomib in MDA-MB-468 cells transfected with scrambled non-silencing siRNA or CaMKK $\beta$  siRNA**

MDA-MB-468 cells, grown in a 6-well plate, were transiently transfected with either 10 nM CaMKK $\beta$  siRNA or scrambled non-silencing siRNA for 60 hours, followed by treatment with 10 nM bortezomib for up to 8 hours. Untreated cells were used as controls. Cell extracts were used for the determination of CT-like activities. Measurements of CT-like activity were performed twice. Each individual experiment was tested in triplicates and the error bars represent the standard deviation.

### **Bortezomib treatment increases newly synthesized CaMKK $\beta$ protein levels**

The accumulation of CaMKK $\beta$  after bortezomib treatment suggests that either CaMKK $\beta$  is a proteasome substrate (hence proteasome inhibition leads to its accumulation) or its protein synthesis is upregulated by a proteasome inhibitor. To investigate the involvement of newly CaMKK $\beta$  protein synthesis after bortezomib treatment, we used cycloheximide, a protein synthesis inhibitor<sup>276</sup>. When MDA-MB-468 cells were co-treated with bortezomib and cycloheximide, an inhibition in levels of pAMPK (but not total AMPK) and ubiquitinated proteins was observed, as compared to bortezomib alone treatment (Figure 8A). To investigate whether bortezomib could also increase levels of CaMKK $\beta$  transcription, qPCR assay was done to assess CaMKK $\beta$  mRNA levels in bortezomib- or solvent-treated MDA-MB-468 cells. We found that bortezomib treatment did not increase, instead decreased levels of CaMKK $\beta$  RNAs by about 50% in MDA-MB-468 breast cancer cells (Figure 8B). Therefore, bortezomib treatment increases CaMKK $\beta$  protein synthesis which correlates with increased AMPK activation in human breast cancer cells.

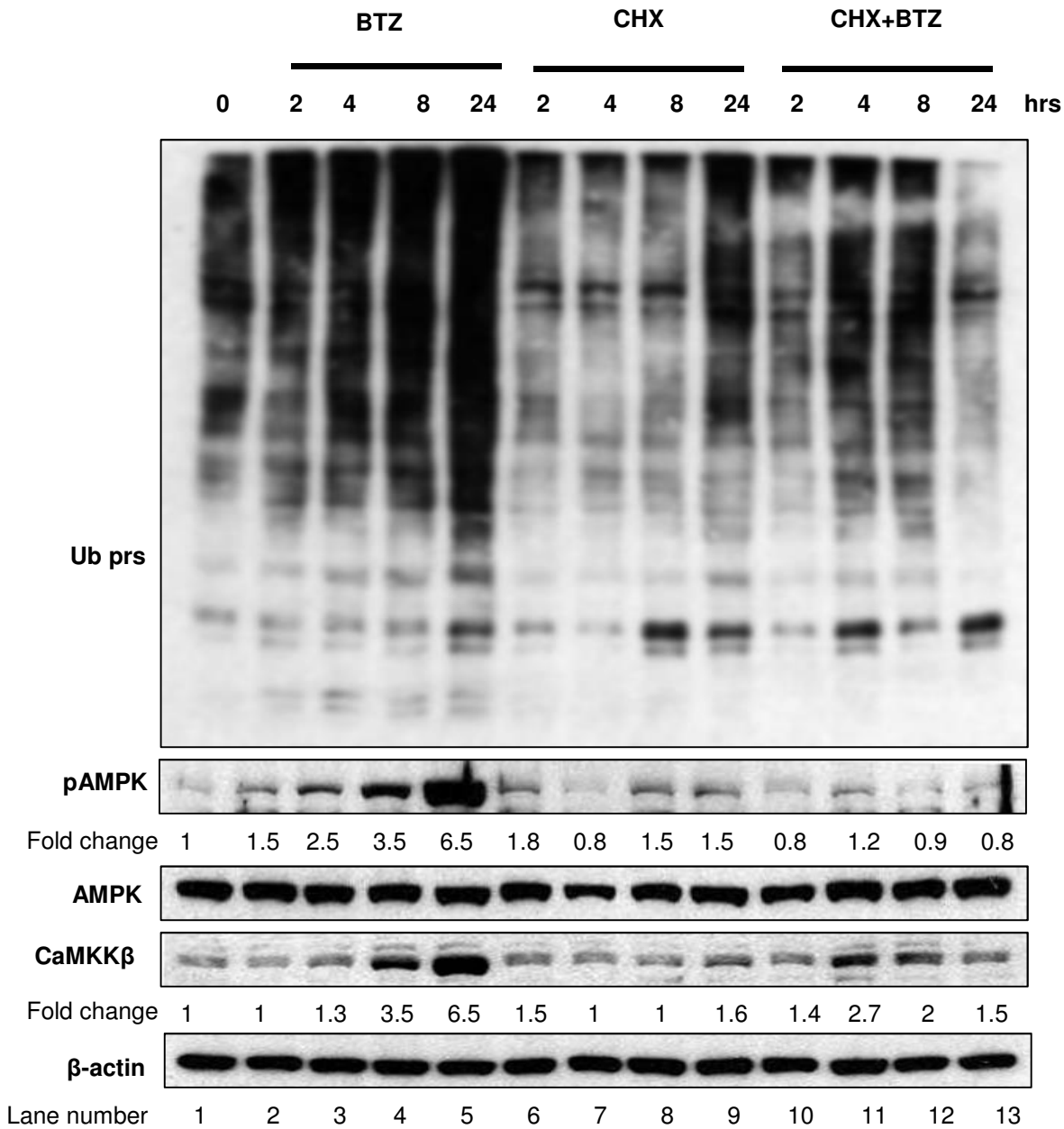
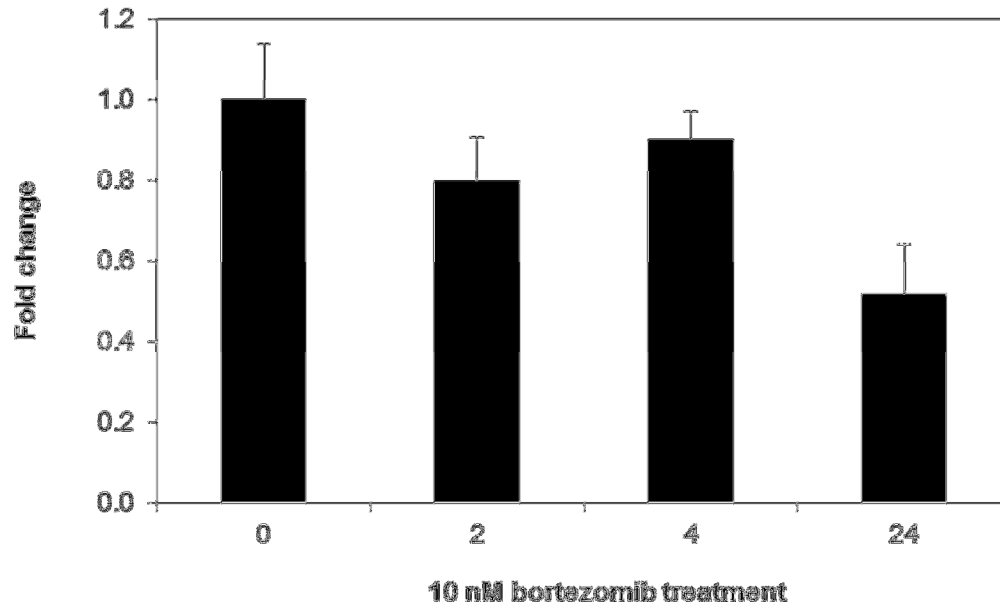


**Figure 8A: Bortezomib increases newly synthesized CaMKK $\beta$  protein levels**

MDA-MB-468 breast cancer cells were treated with 10 nM bortezomib with or without 100 $\mu$ M cycloheximide for up to 24 hours. Cell extracts were used for Western blotting with specific antibodies for pAMPK, AMPK, CaMKK $\beta$ , ubiquitin and  $\beta$ -actin. The data showed in Figure 8A is a representative of three independent experiments. Fold increase in pAMPK/AMPK and CaMKK $\beta$ /  $\beta$ -actin ratio was calculated based on densitometry for the specific blots presented here.



10nM Bortezomib treatment (hours)	Mean Ct	Std Dev Ct	Fold change
0	22.33764	0.11512744	1
2	22.29363	0.19058433	0.798090603
4	21.99215	0.058925	0.901753662
24	22.97031	0.10401905	0.518944717

0	GAPDH	14.42075	0.16530675
2	GAPDH	14.05136	0.05724622
4	GAPDH	13.92607	0.09392042
24	GAPDH	14.10707	0.31788403

**Figure 8B: qPCR assay to assess CaMKK $\beta$  mRNA levels in bortezomib- or solvent-treated MDA-MB-468 cells**

MDA-MB-468 breast cancer cells were treated with 10 nM bortezomib for up to 24 hours, total RNA was isolated, reverse transcribed to complementary DNA and measured by quantitative real-time PCR. Data was normalized to GAPDH. These results were obtained for a preliminary experiment where the standard deviation was calculated from the PCR replicates of the same cDNA preparation. These results supports with the idea that bortezomib treatment increases CaMKK $\beta$  protein synthesis.

## Discussion

The goal for this study was to determine the mechanism of proteasome inhibitor-induced AMPK activation in human breast cancer cells. It has been reported that AMPK has three major upstream kinases: LKB1, CaMKK $\beta$ , and TAK1, each of which is activated in different tissues, by variety of stimuli resulting in diverse outcomes<sup>207,277</sup>. Furthermore, the possibility of crosstalk between AMPK and UPS adds another layer of complexity to the system<sup>278-282</sup>. Considering the importance of AMPK and UPS signaling as two major anticancer strategies, it is important to understand their crosstalk. Indeed, while either AMPK or UPS signaling is well understood, their crosstalk is still unclear. Also, the AMPK regulation by the UPS and *vice versa* forms the basis of an integrated system that connects proteasome-mediated protein degradation and cellular energetics<sup>283,284</sup>. It should be noted that, depending on the target protein or context, a significant amount of cellular energy is spent by the UPS in regulating protein turnover<sup>285-287</sup>.

Our data suggests that AMPK is activated when the proteasome is inhibited irrespective of proteasome inhibitor or cancer cell type (Figure 3). Proteasomal inhibition (Figures 3-5) led to a subsequent rise in intracellular calcium that appears to regulate AMPK activity (Figure 6A-B). The observations detailed in this research project support a model described (Figure 9) whereby CaMKK $\beta$  is the key regulator of AMPK activation by proteasome inhibition. It is also noteworthy that inhibition of AMPK activation by either inhibition of CaMKK $\beta$  itself or calcium chelation led to a significant decrease in accumulation of ubiquitinated proteins (Figures 4A and C as well as 6A and C compare lanes 3 and 9, also Figure 7 compare lanes 3 and 7). Other researchers have also found that bortezomib induces autophagy *via* AMPK activation in myeloma as well as pancreatic and colorectal cancer cells<sup>280,282</sup>. Our finding of AMPK activation by proteasome inhibitors in breast cancer cells are in accordance with them. Although we have not studied whether autophagy is induced by AMPK activation or not as well as the consequences of AMPK

activation, we have tried to decipher the mechanism for AMPK activation mediated by proteasome inhibitors in breast cancer cells.

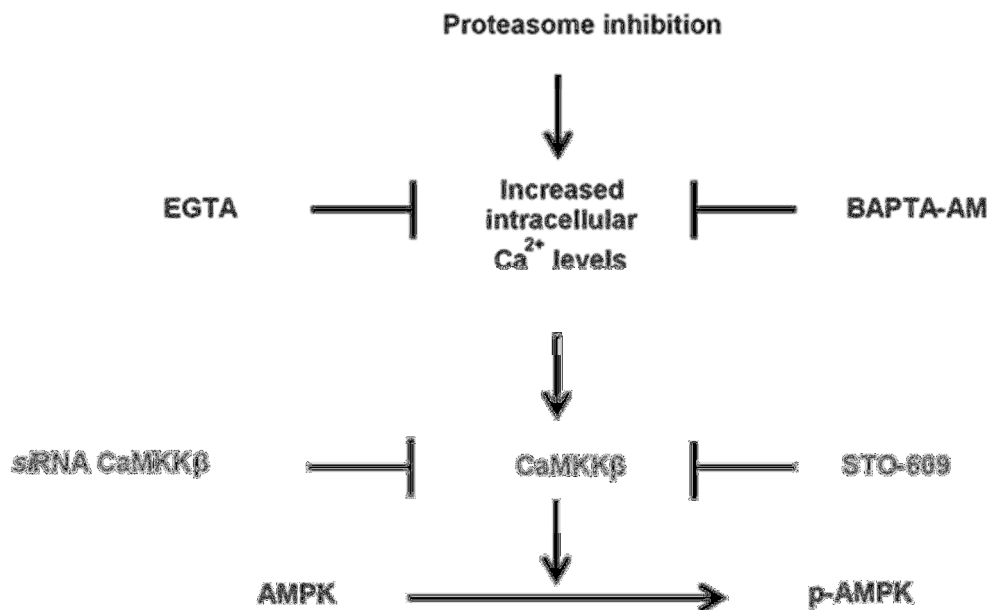


**Figure 9: Proposed schematic for AMPK activation due to proteasome inhibitors**

The cartoon depicts the proposed signaling events starting from the proteasome inhibition induced elevated intracellular calcium ion levels, leading to  $\text{Ca}^{+2}$ -CaMKK $\beta$  cascade resulting in AMPK activation in cancer cells.

Interestingly we also found that treatment with AMPK activators such as metformin and sodium salicylate resulted in accumulation of ubiquitinated proteins in breast cancer cells (Figure10), further supporting the connection of the two antitumor targets, AMPK and UPS. However, further in depth experiments to interrogate the crosstalk and its functional significance in cancer development and treatment are needed. Along this line, some researchers have reported that AMPK activation by proteasome inhibition is involved in compensatory activation of autophagy<sup>288-290</sup>



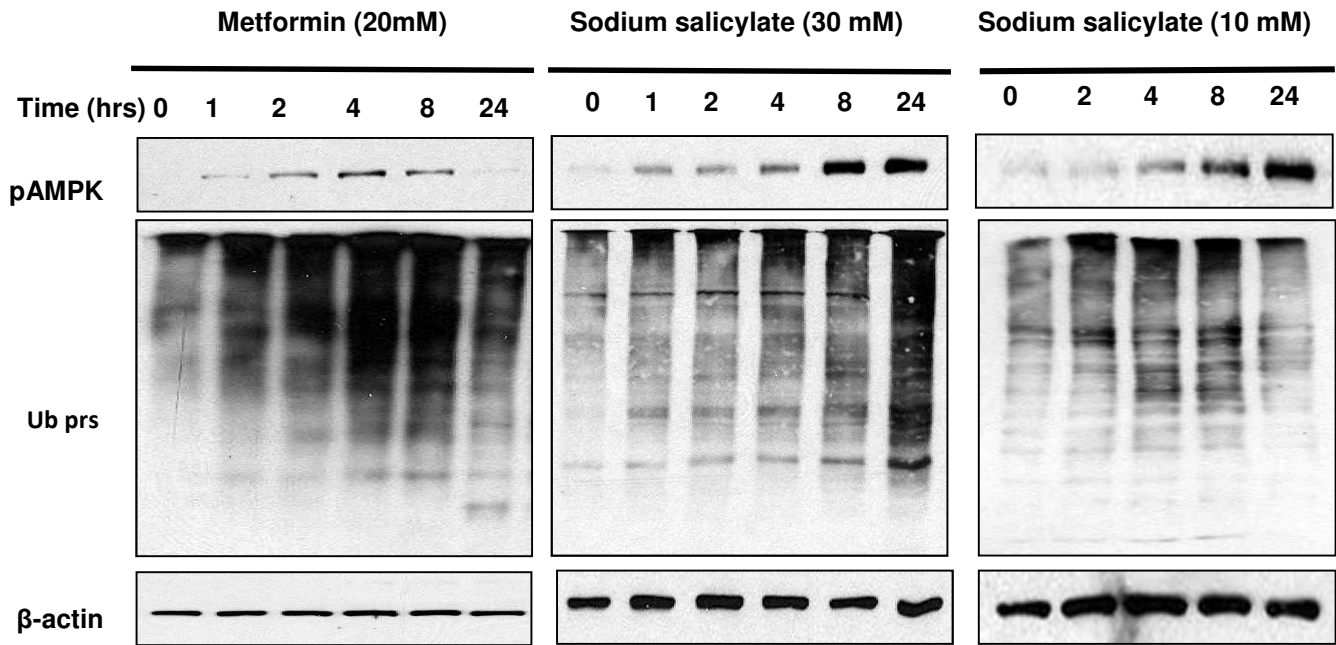


**Figure 10: AMPK activators induce accumulation of ubiquitinated proteins in breast cancer cells**

MDA-MB-231 breast cancer cells were treated with 20 mM metformin (A) or 30 mM sodium salicylate (B) or MDA-MB-468 breast cancer cells were treated with 10 mM sodium salicylate (C) for up to 24 hours. Cell extracts were used for Western blot analysis with specific antibodies for pAMPK, AMPK, ubiquitin and  $\beta$ -actin. The data showed in Figure 10A is a representative of two independent experiments. The data showed in Figure 10B is representative of three independent experiments. The data showed in Figure 10C is a representative of two independent experiments.

We hope that our current findings could further stimulate the collaborations between basic researchers studying protein and energy homeostasis, resulting in elucidation of the mechanism for crosstalk between UPS and AMPK. Additionally, clearer understanding for the mechanism of crosstalk between AMPK and UPS in context of proteasome inhibition and cancer might be helpful in designing novel strategies to overcome resistance to proteasome inhibitors. It has been shown that curcumin has proteasome-inhibitory potential<sup>291</sup> as well as the ability to improve insulin resistance in many rodent models and delay development of type 2 diabetes<sup>292,293</sup>. The proteasome inhibitors also have potential for the treatment of ischemia and reperfusion injury<sup>294</sup>. Therefore, further in depth studies in laboratories as well as clinics are warranted to study AMPK-UPS crosstalk so that novel treatments could be designed for various pathological conditions such as cancer, metabolic disorders as well as ischemia and reperfusion injury.

## CHAPTER 4

### **P-Glycoprotein inhibition sensitizes human breast cancer cells to proteasome inhibitors**

*Adapted from manuscript submitted to International Journal of Molecular Sciences*

Drug resistance is the major problem in successful cancer treatment. As stated earlier, resistance to chemotherapeutic agents could be inherent or acquired<sup>295</sup>. Different mechanisms of chemoresistance include alteration in influx or efflux of drug, inactivation of chemotherapeutic agents, alterations in the target molecules and regulation cell death, enhanced growth factor signaling and DNA repair and aberrant activation of NF- $\kappa$ B signaling<sup>296</sup>. Therefore, chemoresistance must be approached with multiple strategies by using a combination of variety of drugs, which would simultaneously target different mechanisms of chemoresistance.

It has been shown that calcium homeostasis is perturbed due to proteasome inhibition<sup>274,275,297</sup>. We wanted to test whether calcium channel blockers could sensitize breast cancer cells especially triple negative breast cancer cells. Additionally, some calcium channel blockers such as verapamil also inhibit drug efflux pumps as well as drug metabolizing cytochrome P450 enzymes<sup>298,299</sup>. Since concentration of antineoplastic agents inside the cancer cell must be above specific threshold level to show its therapeutic effect, alterations in the influx or efflux of drugs can contribute to chemoresistance. Certain transmembrane transporters are actively involved in efflux of chemically diverse drugs<sup>300</sup>. One of such most important transporters is multidrug resistance protein, MDR1, also called P-gp<sup>301,302</sup>. It is a product of MDR1 gene in human and a first member found in the large family of ATP dependent transporters called ATP-binding cassette family. MDR1 is involved not only in drug efflux but also moving in and out different nutrients and amino acids. It is widely expressed in many human cancer cells. MDR1 can detect and bind to large variety of neutral and hydrophobic anticancer and other therapeutic agents due to its promiscuity<sup>300</sup>. Therefore, concomitant use of

MDR1 inhibitors like verapamil hydrochloride with anticancer agents can be used to reverse multidrug resistance in cancer and chemosensitize cancer cells<sup>303</sup>. Chemosensitization is one of the strategies to overcome resistance with the use of one drug to enhance the efficiency of another by modifying one or more underlying causes of chemoresistance<sup>301</sup>. Therefore, we decided to test whether proteasome inhibitors could be combined with verapamil and nicardipine to further sensitize TNBC cells.

## RESULTS

### Verapamil combination with MG132 shows enhanced cytotoxicity accompanied by increased proteasome inhibition

The objective of this study was to test the effect of combining the P-gp inhibitor verapamil with proteasome inhibitors in TNBC cells. MG132 is an earlier generation of proteasome inhibitor<sup>304</sup>. We exposed MDA-MB-231 cells to different concentrations of MG132 alone, verapamil alone, or their combinations. Results are depicted as boxplots representing the median values and interquartile ranges of percentage relative cell proliferation of MDA-MB-231 cells exposed to MG132, verapamil, and combination, respectively (Figure 11A). The combination of MG132 and verapamil (Mean±SD of % relative cell proliferation, hereafter: 59.30±39.42) showed significantly increased levels of inhibition of cell proliferation in MDA-MB-231 cells, compared to each treatment alone (vs. MG132: 84.19±20.88, adjusted *P* value < 0.0001; vs. verapamil: 71.93±36.12, adjusted *P* value = 0.03). Similarly, the results show that the combination of MG132 and verapamil (67.95±28.49) significantly increases inhibition of cell proliferation in MCF7 cells, compared to each treatment alone (vs. MG132: 100.54±14.37, adjusted *P* value < 0.0001; vs. verapamil: 83.20±27.54, adjusted *P* value = 0.0001; Figure 11B). The detailed statistical analyses for figure 11A and 11B are shown (Figure 11). Furthermore, the combination treatment showed morphological changes indicating apoptosis in the MDA-MB-231 cells (Fig. 11C).

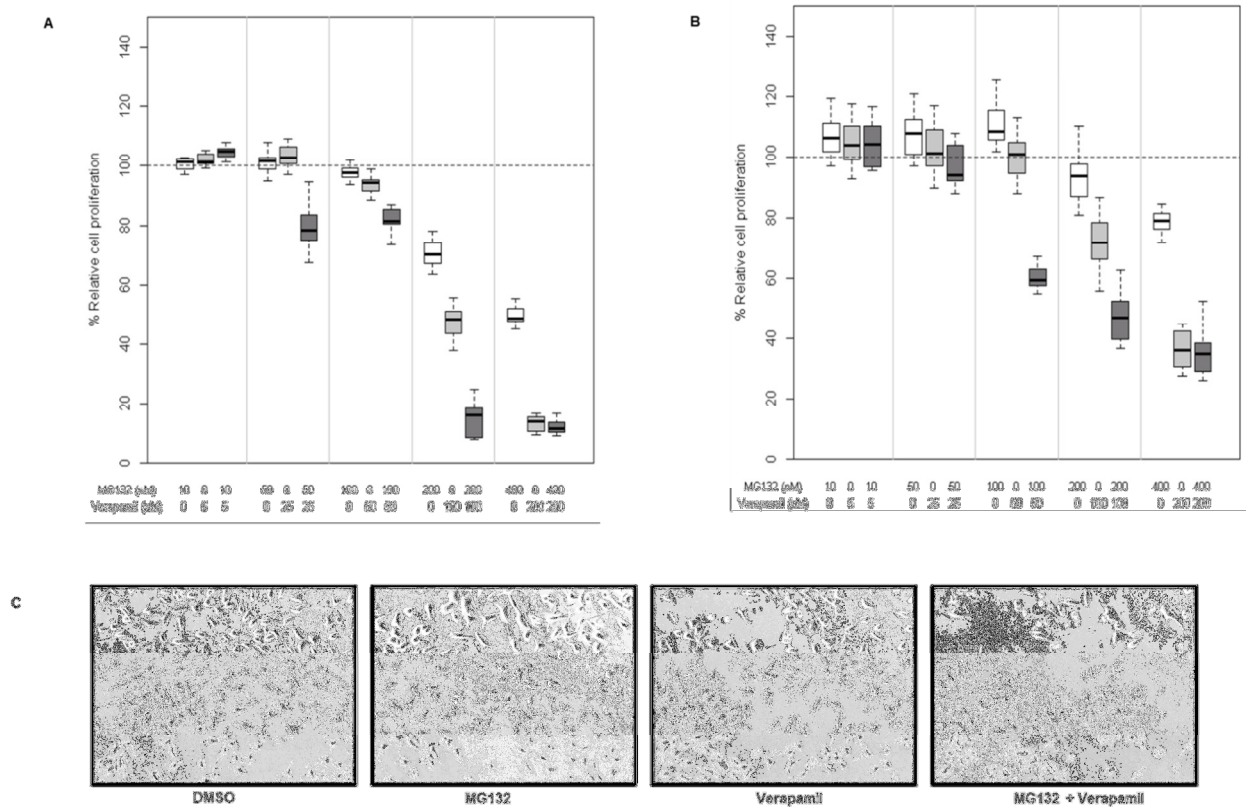


**Figure 11: Verapamil potentiates cytotoxic activities of MG132 in MDA-MB-231 cells.**

(A) Boxplots of percentage relative cell proliferation of MDA-MB-231 cells exposed to MG132, verapamil, or combination, respectively. Median values and interquartile ranges are depicted in boxplots. The dotted horizontal line indicates the relative cell proliferation of 100% as a reference. The means and standard deviations (SD) are further calculated, as shown in Figure 11 continued. These experiments were repeated three times with 5 to 8 replicates for each treatment. (B) Boxplots of percentage relative cell proliferation of MCF7 breast cancer cells exposed to MG132, verapamil, or combination, respectively. Median values and interquartile ranges are depicted in boxplots. The dotted horizontal line indicates the relative cell proliferation of 100% as a reference. The means and standard deviations (SD) are as shown in Figure 11 continued. These experiments were repeated twice with 5 to 8 replicates for each treatment. (C) Detection of morphological changes in MDA-MB-231 cells after treatment with 200 nM MG132, 70 μM verapamil and their combination. MDA-MB-231 cells were treated with different concentrations of

denoted agent either alone or their combinations for 24 hours and morphological changes were detected using phase contrast microscope. The data shown in Figure 13C is representative of 2 independent experiments.

(B)

		Dosing plan															Overall		
		Dosing1			Dosing2			Dosing3			Dosing4			Dosing5			Drug1	Drug2	Combination
Drug1	MG132 (nM)	10	0	10	50	0	50	100	0	100	200	0	200	400	0	400			
Drug2	Verapamil (uM)	0	5	5	0	25	25	0	50	50	0	100	100	0	200	200			
<b>Summary by dosing plan</b>																			
Mean		<b>100.97</b>	102.01	106.07	101.02	103.05	<b>78.63</b>	97.98	93.76	<b>84.36</b>	70.92	47.57	<b>14.18</b>	50.07	<b>13.25</b>	13.28	84.19	71.93	<b>59.30</b>
SD		2.60	1.87	6.41	3.32	3.73	6.60	3.30	2.75	13.84	4.31	5.28	5.65	3.83	2.65	6.51	20.88	36.12	39.42
N		16	16	16	16	16	16	16	16	16	16	16	16	16	16	16	80	80	80
Mean: mean of % relative cell proliferation; SD: standard deviation; N: sample size																			
Bold italic numbers: the minimum mean % relative cell proliferation																			
<b>Statistical testing</b>																			
		ANOVA by dosing plan															Overall ANOVA		
		Dosing1		Dosing2		Dosing3		Dosing4		Dosing5		Overall							
		p-value1	p-value2	p-value1	p-value2	p-value1	p-value2	p-value1	p-value2	p-value1	p-value2	p-value1	p-value2						
Overall		<b>0.0011</b>	<b>0.0007</b>	<b>0.0000</b>	<b>0.0000</b>	<b>0.0000</b>	<b>0.0000</b>	<b>0.0000</b>	<b>0.0000</b>	<b>0.0000</b>	<b>0.0000</b>	<b>0.0000</b>	<b>0.0012</b>						
		Pairwise post-hoc by dosing plan															Overall pairwise post-hoc		
Drug 1 vs. Drug 2		0.4806	0.1809	0.2350	0.1366	0.1602	<b>0.0009</b>	<b>0.0000</b>	<b>0.0000</b>	<b>0.0000</b>	<b>0.0000</b>	<b>0.0000</b>	<b>0.0000</b>	<b>0.0335</b>	0.1749				
Drug 1 vs. Combination		<b>0.0033</b>	<b>0.0026</b>	<b>0.0000</b>	<b>0.0000</b>	<b>0.0001</b>	<b>0.0001</b>	<b>0.0000</b>	<b>0.0000</b>	<b>0.0000</b>	<b>0.0000</b>	<b>0.0000</b>	<b>0.0000</b>	<b>0.0000</b>	<b>0.0017</b>				
Drug 2 vs. Combination		<b>0.0161</b>	<b>0.0062</b>	<b>0.0000</b>	<b>0.0000</b>	<b>0.0054</b>	<b>0.0001</b>	<b>0.0000</b>	<b>0.0000</b>	<b>0.9824</b>	0.2206	<b>0.0335</b>	<b>0.0237</b>						
p-value1: p-values from ANOVA, and p-values of pairwise post-hoc t-test are adjusted by Holm's method																			
p-value2: p-values from Kruskal-Wallis test, and p-values of pairwise post-hoc Wilcoxon test are adjusted by Holm's method																			
Bold italic numbers: significant at the 5% level																			
<b>The analyses and interpretation are based mainly on p-value1 (ANOVA), and as a reference, those of p-value2 (KW) are also included.</b>																			

		Dosing plan															Overall		
		Dosing1			Dosing2			Dosing3			Dosing4			Dosing5			Drug1	Drug2	Combination
Drug1	MG132 (nM)	10	0	10	50	0	50	100	0	100	200	0	200	400	0	400			
Drug2	Verapamil (uM)	0	5	5	0	25	25	0	50	50	0	100	100	0	200	200			
<b>Summary by dosing plan</b>																			
Mean		107.95	105.12	<b>100.4</b>	107.97	102.62	<b>97.3</b>	110.75	100.28	<b>60.2</b>	93.59	71.61	<b>47</b>	82.42	36.34	<b>34.9</b>	100.54	83.2	<b>67.95</b>
SD		8.75	7.32	18.85	8.15	7.64	6.68	6.89	6.89	3.82	8.11	9.48	8.31	14.17	5.77	7.09	14.37	27.54	28.49
N		16	16	16	16	16	16	16	16	16	16	16	16	16	16	16	80	80	80
Mean: mean of % relative cell proliferation; SD: standard deviation; N: sample size																			
Bold italic numbers: the minimum mean % relative cell proliferation																			
<b>Statistical testing</b>																			
		ANOVA by dosing plan															Overall ANOVA		
		Dosing1		Dosing2		Dosing3		Dosing4		Dosing5		Overall							
		p-value1	p-value2	p-value1	p-value2	p-value1	p-value2	p-value1	p-value2	p-value1	p-value2	p-value1	p-value2						
Overall		<b>0.0975</b>	0.5020	<b>0.0002</b>	<b>0.0012</b>	<b>0.0000</b>	<b>0.0000</b>	<b>0.0000</b>	<b>0.0000</b>	<b>0.0000</b>	<b>0.0000</b>	<b>0.0000</b>	<b>0.0000</b>						
		Pairwise post-hoc by dosing plan															Overall pairwise post-hoc		
Drug 1 vs. Drug 2		0.6022	0.9000	0.0999	0.0549	<b>0.0000</b>	<b>0.0005</b>	<b>0.0000</b>	<b>0.0000</b>	<b>0.0000</b>	<b>0.0000</b>	<b>0.0000</b>	<b>0.0000</b>	<b>0.0000</b>	<b>0.0002</b>				
Drug 1 vs. Combination		0.3032	0.9000	<b>0.0006</b>	<b>0.0022</b>	<b>0.0000</b>	<b>0.0000</b>	<b>0.0000</b>	<b>0.0000</b>	<b>0.0000</b>	<b>0.0000</b>	<b>0.0000</b>	<b>0.0000</b>	<b>0.0000</b>	<b>0.0000</b>				
Drug 2 vs. Combination		0.6022	0.9000	0.0999	0.0549	<b>0.0000</b>	<b>0.0000</b>	<b>0.0000</b>	<b>0.0000</b>	<b>0.0000</b>	<b>0.0000</b>	0.6741	0.3365	<b>0.0001</b>	<b>0.0012</b>				
p-value1: p-values from ANOVA, and p-values of pairwise post-hoc t-test are adjusted by Holm's method																			
p-value2: p-values from Kruskal-Wallis test, and p-values of pairwise post-hoc Wilcoxon test are adjusted by Holm's method																			
Bold italic numbers: significant at the 5% level																			
<b>The analyses and interpretation are based mainly on p-value1 (ANOVA), and as a reference, those of p-value2 (KW) are also included.</b>																			

Figure 11 (continued): Verapamil potentiates cytotoxic activities of MG132 in MDA-MB-231 cells. Statistical analyses for Figure 11A and B.

To study the effect on proteasome, MDA-MB-231 cells were treated with either 200 nM MG132 alone (Figure 12A), 70  $\mu$ M verapamil alone (Figure 12B), or their combination (Figure 12C); we observed enhanced proteasome-inhibitory (increased levels of ubiquitinated proteins, p27 and I $\kappa$ B $\alpha$ ) and apoptotic (PARP cleavage) effects in the combination setting, compared to each alone. Increased levels of ubiquitinated proteins and proteasomal target proteins, p27 and I $\kappa$ B $\alpha$  by verapamil alone (Figure 12B) suggests its proteasome-inhibitory function.



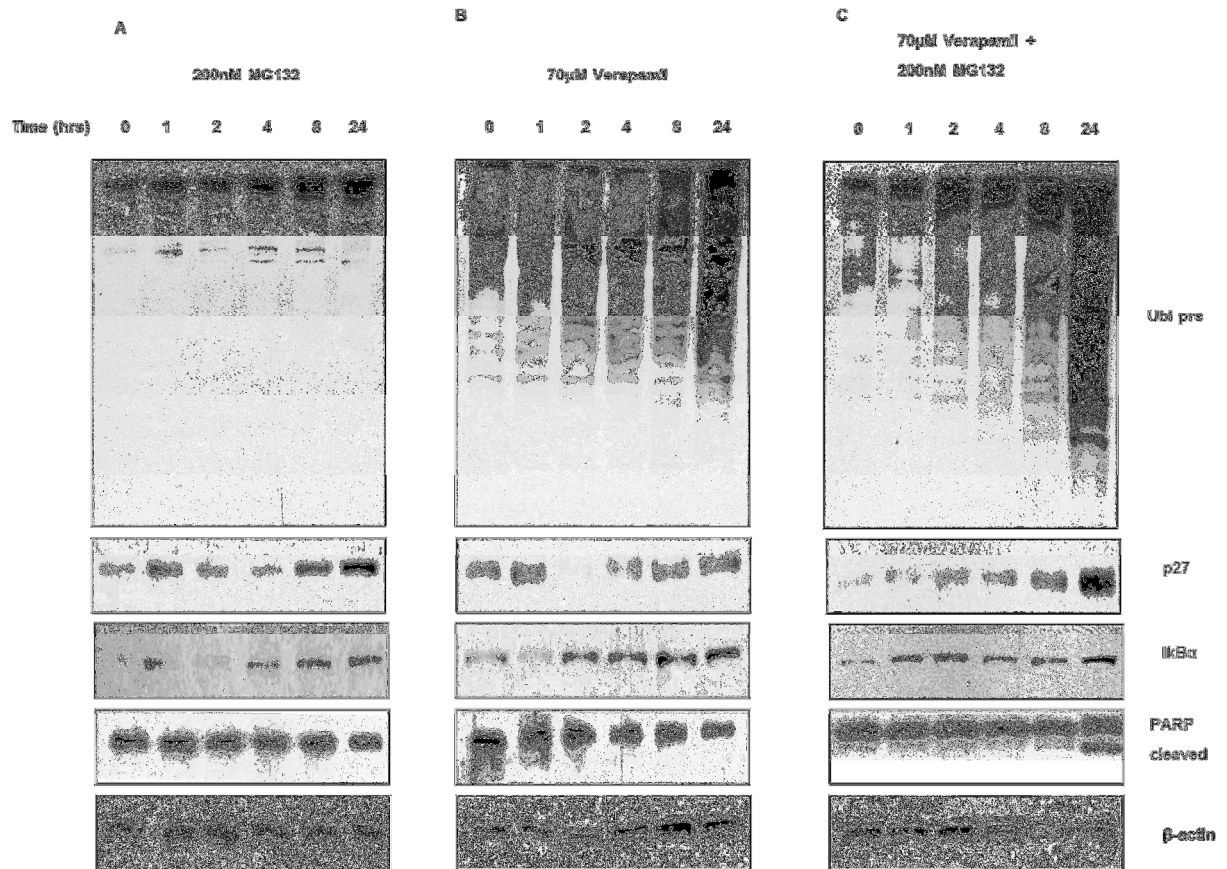


**Figure 12: Verapamil potentiates proteasome-inhibitory activities of MG132 in MDA-MB-231 cells.** MDA-MB-231 cells treated with 200 nM MG132 (A), 70  $\mu$ M verapamil alone (B) or their combination (C) for 24 hours, followed by preparation of whole cell extract and Western blot analysis using specific antibodies for ubiquitin, I $\kappa$ B $\alpha$ , p27<sup>kip1</sup> and PARP, with  $\beta$ -actin as loading control. The data showed in Figure 12 is a representative of two independent experiments.

### Enhanced cytotoxic activity of bortezomib and verapamil combination on TNBC cells

We then tested if verapamil could potentiate proteasome-inhibitory properties of structurally different and US FDA approved proteasome inhibitors. First, we systematically compared the inhibitory effect of different concentrations of bortezomib and verapamil alone and their combinations in TNBC MDA-MB-231 cells by using cell viability assay, MTT. The combination of bortezomib and verapamil ( $54.10 \pm 31.46$ ) showed increased levels of growth inhibition in MDA-MB-231 cells, compared to each treatment alone, but the inhibition level of the combination was not significant compared to that of bortezomib (vs. bortezomib:  $57.89 \pm 25.25$ , adjusted  $P$  value = 0.42; vs. verapamil:  $76.11 \pm 22.27$ , adjusted  $P$  value < 0.0001; Figure 13A). Importantly, bortezomib and verapamil co-treatment specifically at the dose of 10 nM and 50  $\mu$ M ( $51.87 \pm 5.76$ ) showed enhanced growth inhibition as compared to each treatment alone in these cells (vs. bortezomib:  $58.77 \pm 4.80$ , adjusted  $P$  value = 0.0006; vs. verapamil:  $94.56 \pm 5.30$ , adjusted  $P$  value < 0.0001; Figure 13A), supporting the idea that P-gp inhibition might sensitize these TNBC cells to proteasome inhibitors. We then tested whether the MDA-MB-231 cells treated with bortezomib and verapamil combination were undergoing apoptosis using the CellEvent Caspase-3/7 green detection reagent (Invitrogen). We detected more apoptotic cells after co-treatment with the combination of bortezomib and verapamil than each agent alone (Figure 13B) In order to find out the mechanism for the enhanced activity, we studied the effect of the verapamil and bortezomib combination on proteasome substrates and apoptosis biomarkers (Figure 13). We observed increased accumulation of ubiquitinated proteins which indicates higher levels of proteasome inhibition after treatment with the combination (Figure 13D) compared to verapamil (Figure 12B) and bortezomib alone (Figure 13C). It has been reported that inhibition of the NF- $\kappa$ B pathway is partially responsible for cytotoxic effect by bortezomib. It occurs through stabilization of the endogenous inhibitor, I $\kappa$ B $\alpha$ , a proteasome substrate, resulting in sequestration of NF- $\kappa$ B in the cytoplasm. This leads to prevention of